Master's thesis

NTNU
Norwegian University of Science and Technology
Faculty of Engineering
Department of Manufacturing and Civil Engineering

Petter Vang

Simulation Validation of Extruded Aluminium Quenching

Master's thesis in Production and product development
Supervisor: Jun Ma
Co-supervisor: Eren Can Sariyarlioglu
June 2023

NTNU
Norwegian University of
Science and Technology

Petter Vang

Simulation Validation of Extruded Aluminium Quenching

Master's thesis in Production and product development
Supervisor: Jun Ma
Co-supervisor: Eren Can Sariyarlioglu
June 2023

Norwegian University of Science and Technology
Faculty of Engineering
Department of Manufacturing and Civil Engineering

NTNU
Norwegian University of
Science and Technology

ABSTRACT

This thesis looks at validating the simulation software QForm made for simulating the processing of hot metals and, more specifically, looking at the extrusion and quenching part of the software. This will be done by recreating a test done by the company Benteler in software as closely as possible and comparing the results to the data gathered from the tests. The aluminium profile used in these tests and simulations is made in alloy 6005, and the dies are made from H13 tool steel.

For the extrusion part, the comparison data relies mainly on the force and temperature data, as there was no distortion or other reliable data available to conclude from, though they are the most telling data to go off of.

As for the quenching simulations, there is only the temperature data available, but this is the most important data type, and it is a rather large data set, so there are data to go off of.

Denne masteroppgaven ser på å validere simuleringene gjort i programvaren QForm som er laget for å simulere forming av varmt metall, og spesielt ekstrudering og kjøle simuleringer. Denne valideringen vil bli gjort ved å gjenskape tester som Benteler har gjort i QFrom og sammenligne resultatene mellom testene og simuleringene. Testene ble gjort med 6005 som ekstruderings materiale og H13 verktøy stål for former.

For ekstruderingsdelen, dataen som blir sammenlignet vil være av kraften i pressen og temperaturen på metallet når det er kommet ut av formen. Forvrengningene i profilen kan dessverre ikke sammenlignes på grunn av mangel på data.

Og for kjøle simuleringene blir det å sammenligne temperatur grafene for mange forskjellige tester, også her mangler det data på forvrengning.

PREFACE

This thesis will look at using the simulation software QForm to optimize the cooling of extruded aluminium as it comes out of the extrusion press. This cooling is usually done with water and air, where water gives much faster cooling but can give distorted extrudates. On the other hand, while air even cools the profile, keeping them straight, this slower cooling can cause a loss of hardness and strength in the beam.

Aluminium alloys behave significantly differently concerning cooling requirements after forging, casting and extrusions to get suitable mechanical properties. These differences set some initial conditions for what kind of cooling is required. Some alloys get the proper mechanical strength without quenching (rapid cooling, typically with water). Others are quench-sensitive and have wildly different mechanical properties depending on how fast they are cooled during quenching.

Given the dynamic nature of quenching and rapid changes in metal, there are ample possibilities of getting uneven cooling on different parts of a profile. This unevenness typically leads to distorted beams, making them useless or needing to be plastically corrected after the quenching, adding additional processes and costs to the production. With trial, error and experience, this uneven cooling can be corrected, but this process is costly, taking time and using up perfect material that needs to be recycled. This thesis looks into eliminating or significantly reducing by moving these trials into a simulation that only costs some operator time and electrical power.

CONTENTS

LIST OF FIGURES

LIST OF TABLES

ABBREVIATIONS

List of all abbreviations in alphabetic order:

- **BOM** Bill Of Materials
- **CAD** Computer-Aided Design
- **DXF** Drawing Exchange Format
- **FEA** Finite Element Analysis
- **HTC** Heat Transfer Coefficient
- **ICEB** International Conference on Extrusion and Comparison
- **IR** InfraRed
- **NTNU** Norwegian University of Science and Technology
- **STEP** Standard for The Exchange of Product data (ISO 10303)

CHAPTER

ONE

INTRODUCTION

1.1 Motivation

As extrusion is one of the most used production forms for shaping aluminium, optimising it for efficient and productive production is essential. One way of doing this is using software to set up the cooling and quench box instead of going off an educated guess and doing trial and error. One of the reasons this is not being done yet is that it is a complex problem to solve with high-temperature changes, the HTC (heat transfer coefficient) is heavily dependent on the micro surface structure of the profile being cooled, and lastly, to get everything the extrusion process itself should also be simulated to give the proper temperature distribution as in input to the cooling simulation.

1.2 Project Pescription

This is where the simulation software QForm comes in as a tool for the plastic deformation simulation of metals. It has recently added the functionality for extrusion and extrusion quenching, which this thesis will look at and see if it gives good enough results to be used in the industry. If this is the case, it will

allow extrusion production companies to move away from the costly trial-and-error method to a digital simulation for setting up the quenching of extruded profiles while still getting straight and good-quality quenches.

To explore if the software is good enough, this thesis will look at recreating a set of tests done by Benteler in software and compare and contrast the results gathered from the software with the data collected during the real-world test.

1.2.0.1 Stakeholders

This thesis is written with NTNU as the task provider, where Geir Ringen and Jun Ma are supervisors for the master thesis. The company Benteler have done some extrusion tests with different settings and setups in their extrusion quench box. I will replicate these tests in software to see how well the simulation matches the data.

1.3 Why Aluminium

Aluminium is one of the most abundant materials in the earth's crust, after oxygen and silicon. Despite it being this abundant, any naturally occurring metalling aluminium hardly exists. It is bounded by oxygen, silicon or other atoms forming various salts and rocks. Aluminium is mostly obtained from bauxite ore, which consists of aluminium and oxygen bound with some hydroxides and other atoms in smaller amounts. To make metallic aluminium, one starts with bauxite which is first crushed and ground into a fine powder. This powder is then washed to remove impurities and produce alumina, which is then put into electrolysis ovens to produce raw aluminium. Raw aluminium is not all that strong at only 7-11 MPa in yield strength. It needs to be alloyed into stronger alloys to be useful for engineers and others in products and construction. These days the alloys can get up to 600 MPa in yield strength (I.J. 1995). Other useful qualities of aluminium are that it is a ductile metal with an elongation of 50-70%, it is malleable, allowing drawing and extruding, and it is also easily machinable and castable. It also has excellent thermal and electrical conductivity, which is 60% of copper at only 30% of the weight with a density of only $2.70 g/mm^3$ or about 1/3 of steel. However,

it is not quite as stiff as steel, at about 1/3 of steel elastic modulus. (I.J. 1995) Another good reason to use aluminium is that it is easy to recycle and is today the metal with the highest percentage of recycling. Recycling aluminium costs only five percent of the energy required to take it from bauxite to raw aluminium.

1.4 Aluminium Extrusion

The most used materials in extrusion are aluminium, copper, and steel alloys. In this thesis, I will focus on aluminium (also applicable to other metals) as the material for extrusion. Working with aluminium and metals means high forces and temperatures to keep the metal soft enough to be formable. It is possible to do some simple extrusion/forming of aluminium cold, but this limits the forming to minor dimension changes before the material work hardens too much and breaks apart. Extrusion is therefore done over the aluminium annealing temperature, keeping the material malleable and softer. Those high temperatures also reduce the power needed to push the material through the die, increase the speed at which it is possible to press the aluminium through and allow the coss-section changes from a massive billet to the finished profile to be much larger.

Figure 1.4.1: Some extruded profiles in aluminium (*Hydro extruded profiles* 2022)

1.4.1 Aluminium Extrusion

Extrusion can summarise various techniques under the collective noun "extrusion". The name extrusion can be everything from drawing metal blanks into a cylinder to screwing plastics into a mould. When discussing extrusion, the more common thought of manufacturing technique is pressing material, be it plastics or metals, through a die to give it a consistent cross-section over a long beam cut into the desired lengths. In the case of plastics, a specially shaped screw is used to heat and mix the material, while metals are pre-heated to lower strength and inserted as cylinders or hollow cylinders. Below is figure1.4.2 showing the four main types of metal extrusion used in the industry today. Where direct, indirect and hydrostatic takes massive billets, the tubular one takes (or makes) hollow billets. Aluminium extrusion is a standard method of forming aluminium, but it will generate some waste due to the transition between two billets. The remaining end of the first billet contains impurities and oxidation left in the press and needs to be removed. There are also impurities at the front end of the new billet that get pressed into the extrusion, so the first few meters of the extruded profile from the new billet must be cut off and recycled. To optimise the process and reduce waste, removing impurities effectively and improving the transition between billets is essential.

The two lower extrusion types shown in figure 1.4.2 are more specialised extrusion methods. Tubular extrusion makes hollow extrusions without welding, giving a stronger finished product. Still, it is a less productive and more costly extrusion process than direct or indirect. Hydrostatic extrusion has the same disadvantages as tubular extrusion and additional ones such as fluid handling. The billet must be machined before being placed in the press. Because the billets need a taper that matches the die's entry angle and should remove all the surface impurities, the press can extrude more of the billet without getting impurities into the finished profile. Other advantages are a more uniform loading of the billet material, no friction against the walls of the press, and lower peak forces needed, allowing the option to run at lower temperatures. (Saha 2000)

Aluminium extrusions are one of the most used ways of making aluminium products. Aluminium is a strong and lightweight material, making it useful for many tasks.

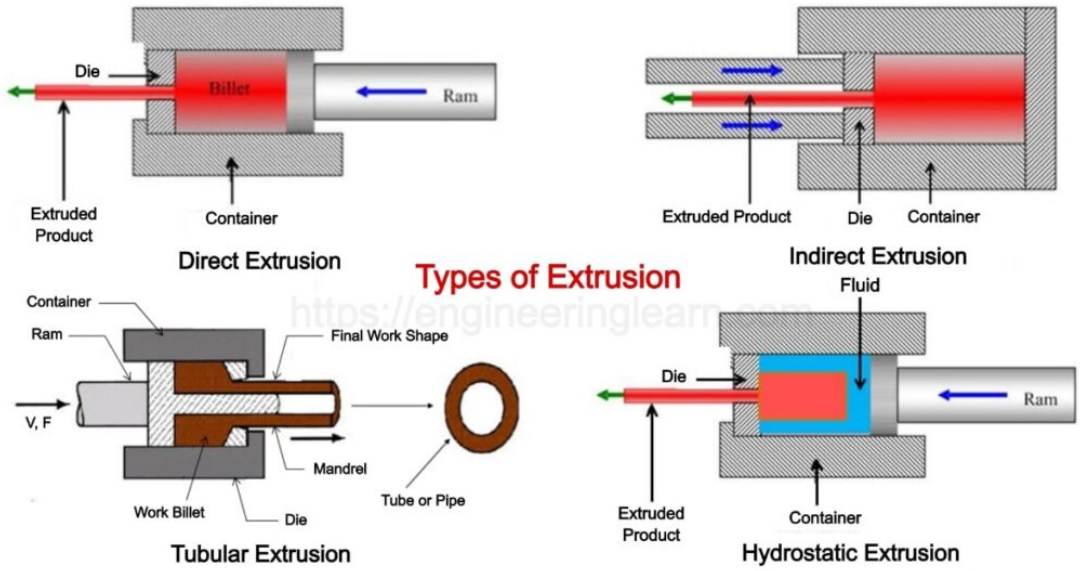

Figure 1.4.2: Figure showing the four main types of continuous extrusion (*File:Extrusion force plot.png - Wikimedia Commons* n.d.)

These properties give light and strong end products, making them both easier to use and, in most cases, more environmentally friendly. They are easier to move around from the lower weight. Another reason they are environmentally friendly is how easy they are to recycle with little energy needed to do the remelting and relatively easy to make a good material out of the recycled material so that it is easy to use in the next cycle. So far, it is only about the material itself, so now, some of the reasons extrusions are so popular and cheap. One of the first reasons is that extrusion is a bulk processing technique that makes it possible to make many products quickly. For example, with a billet that is 500 mm long and an extrusion ratio of 25:1, after doing that extrusion, you have 12 500 mm of the theoretical product. Still, as nothing is 100% effective, there is typically a 15-30% loss in the extrusion process, but that still leaves 8750 mm of a finished product that producers can sell. And that is from one billet on the shorter side. Extrusion is also a fast process with a typical extrusion speed of over five mm/s on the ram when extruding. If the process is optimised, it should only take a few min from one extrusion to the next, making for a high utility of the equipment, which is also usually long-lasting, though with some wearing parts. The parts that need exchanging the oftest are the dies, with the container liners walls and the die support structure being parts that wear but not nearly as high wear.

1.4.2 Extrusion Types

Direct extrusion is one of the two most used types, and the other is indirect extrusion. The defining characteristic of Direct extrusion is the material being pushed towards the die, while indirect extrusion is, on the other hand, the die moving towards the material, as can be seen in figure 1.4.2.

The two main pros and cons of indirect are that it inherently has higher dimensional accuracy, but this is at the cost of lower productivity. These properties come from the material keeping a more steady temperature during the process and a more stable material flow during the operation.

Direct extrusion has a lower inherent dimensional accuracy, but its most prominent selling point is higher productivity (Chahare and Inamdar 2016). These statements have some caveats, with properly controlled process parameters, as it is the real world. With good routines, the finished product from direct extrusion is equally good as the indirect. Still, it is harder to get there though this is well worth it in the industry as they can have much higher productivity with direct extrusion compared to indirect and for those producing parts for a living, that counts much more. Another minor problem with indirect is the limitation in the outer diameter of the extruded profile, have to be smaller than the inside diameter of the hollow ram, as it needs to pass through that opening. The die is also limited by both the outer and inner diameter of the ram, as the walls on the die have to be thick enough to handle the forces, and the inner diameter of the ram dictates the maximum profile size.

1.5 Defects and Quality Problems

1.5.1 Extrusion Defects

When doing extrusion, some defects can occur if the process is not optimised for the extruded profile and material. These include underfilling, streaking lines, insufficient welding quality, back-end defects, charge weld propagation, surface speed cracking and microstructure defects.

Press area defects are examples of bearing washout as seen in figure 1.5.1, where some part of the bearings have been eroded during use, making a small trench in the bearing where the aluminium can flow past, giving a line of too much material on the extruded profile. (Qamar, Arif, and Sheikh 2004)

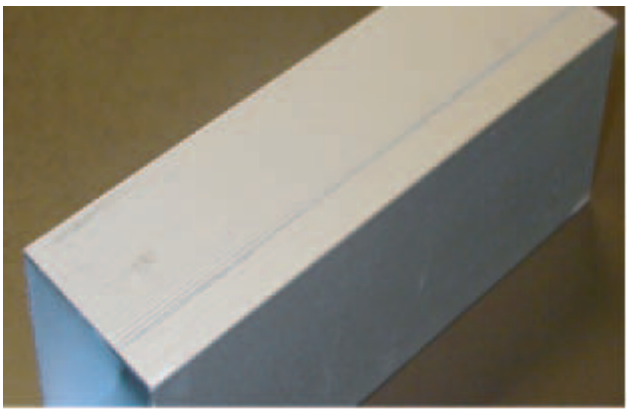

Figure 1.5.1: bearing washout lines in profile (Qamar, Arif, and Sheikh 2004)

Other defects are blistering and blow holes where impurities like lubricants have gotten into the dead-metal zones and down into the product's surface, where they, in later heat treatment processes, expand and make blisters or blow holes as seen in figure 1.5.2.(Qamar, Arif, and Sheikh 2004)

Pick-up defects, characterized by intermittent score lines and pick-up deposits (flecks of aluminium debris), are frequently observed during extrusion. These defects may be caused by including hard particles such as silicon (Si) or magnesium (Mg) in the billet material, leading to high local friction and temperature levels. This material can result in black burn marks, known as silicon marks, on the extruded surface. (Qamar, Arif, and Sheikh 2004)

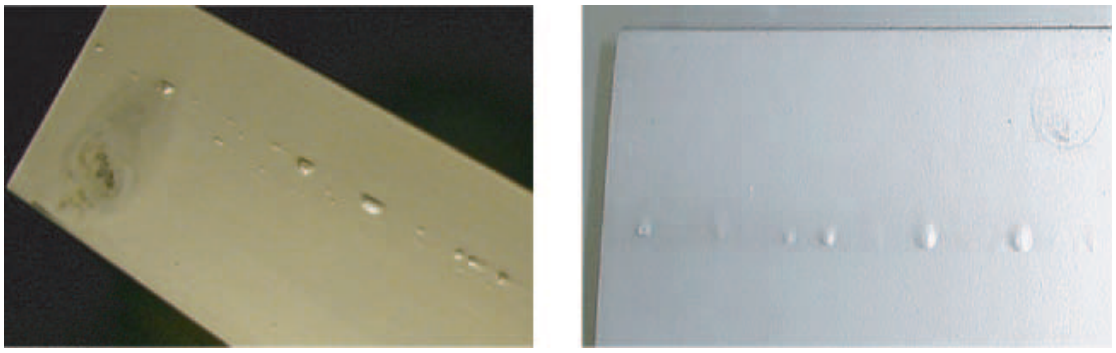

Figure 1.5.2: Blisters (left) and blow holes (right) caused by escaping gases (Qamar, Arif, and Sheikh 2004)

Runout marks, also known as graphite lines, may appear on the extruded surface, particularly in heavy sections, due to friction between the hot extruded material and conveyor rollers made of graphite. These marks are typically longitudinal and may be either carbon or roll marks. If the extrusion process is interrupted, for example, due to a furnace or press component malfunction, die stop marks (band-like patterns perpendicular to the extruded length) may appear on the affected section. (Qamar, Arif, and Sheikh 2004)

In standard practice, one usually runs the billets billet-to-billet, where the back end of the first billet is cut off, and the material inside the die is left there. The next billet is loaded and welded to the end of the billet as seen in figure 1.5.3 on the (left) side. Strains/oil patches come from oil splashed onto the profiles while cutting them to length. This oil then spreads along them before they get burned by the high temperatures. These marks can be seen in figure 1.5.3 right side, where they appear between brown and yellow spots, which may worsen in the ageing furnaces.

Bends and twists happen from uneven metal flow out of the die, getting the effect of the profile getting pushed and bent out of the straight path (see figure 1.5.4 left side). This bending and twisting can also happen from uneven heating of different sides or different cooling of the sides, giving nonuniform temperature distributions. There can also be some ending from poorly done stacking. (Qamar, Arif, and Sheikh 2004)

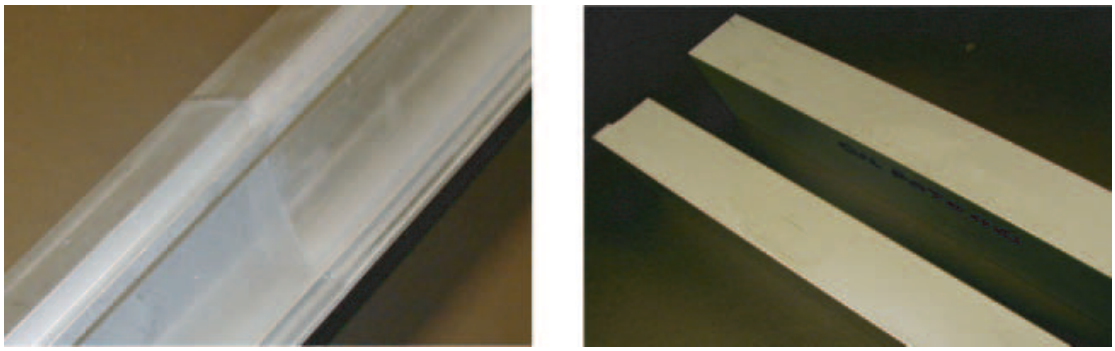

Figure 1.5.3: Transverse weld lines (left) formed from a billet-to-billet joint, and oil patches and strains (right) are caused by surface discolouration (Qamar, Arif, and Sheikh 2004)

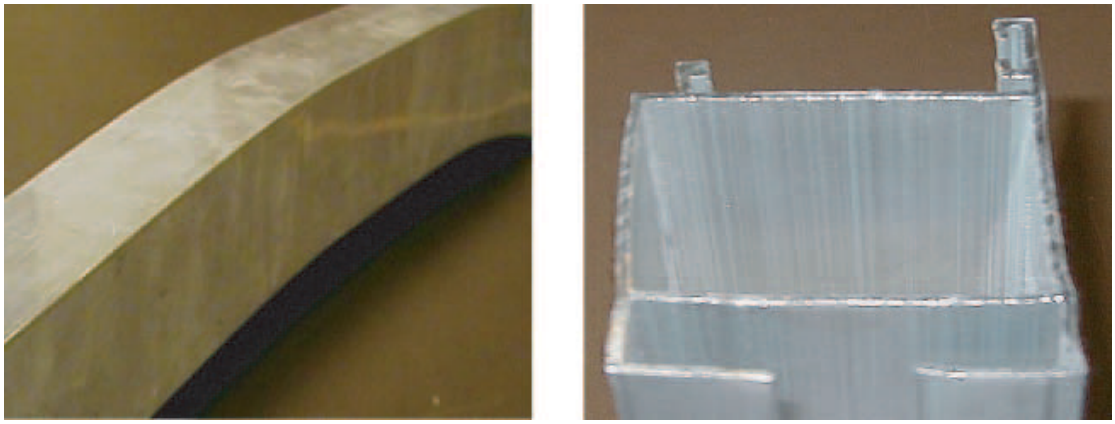

Figure 1.5.4: (left) section that is bent and twisted, (right) out of tolerance profile (Qamar, Arif, and Sheikh 2004)

As with all industries, the extrusion industry also has tolerances that they need to make products within. In figure 1.5.4 right side, one can see one profile with some concave and convex sides, some parts bent out of angle, or just uneven surfaces, that are server enough to be seen on an image. Faults like these often come from variable flow out of the die, they can also happen during stretching, and some of the walls buckle or bend. With dies that have mandrels, it is also possible to get out of the centre, giving the wrong thickness on the profile walls. There are also the usual damages from common collisions and mishaps during transport, stacking and other logistics, like dents, scratches, marks of different sorts and roughened surfaces. (Qamar, Arif, and Sheikh 2004)

1.5.2 Cooling Defects

The two main types of defects from the quenching of aluminium profiles are the beams bending or warping and the other is insufficient quenching.

The first defect is caused by inhomogeneous or too fast cooling causing temperature differences and thermal expansion/contraction at different profile parts. The chance of getting this defect heavily depends on how fast the profile is cooled down and the geometry of the profile itself; see figure 1.5.5. The faster a profile is cooled down, the easier it is to cool some parts of the profile more than other parts, giving temperature gradients and different thermal expansions, which can cause warping of the profile. Cooling down a complex or non-symmetric profile can also cause trouble with different temperatures at different parts of a profile. This is more likely when there are different wall thicknesses at different profile parts, as a thicker wall will cool down slower than a thin wall. In most cases, this warping will become either the beam bending into a banana shape in some direction, the profile twisting along the extrusion direction or a combination of the two.

The other primary defect type is insufficient quenching of the profile giving low mechanical properties, like hardness and yield strength. As seen in figure 1.5.5, there is a window for how fast and slow one can cool a quench-sensitive profile. To fast and one gets defects like in the paragraph above, while too slow, the profile is not quenched, giving a weaker material. This can and most likely will cause problems for the ones using the profile as it is not as strong or hard as it should be and can break during use. On the other hand, if the profile is cooled too fast, there can be distortions or internal stresses, creating problems later.

1.5.3 Objective and Scope

The objective of this master is to look at the feasibility of using software to dial in a quenching and cooling box for aluminium extrusions instead of doing trial and error testing to get the quenching inside acceptable tolerances for the extrude. The first step is figuring out if the software is good enough to get the same results

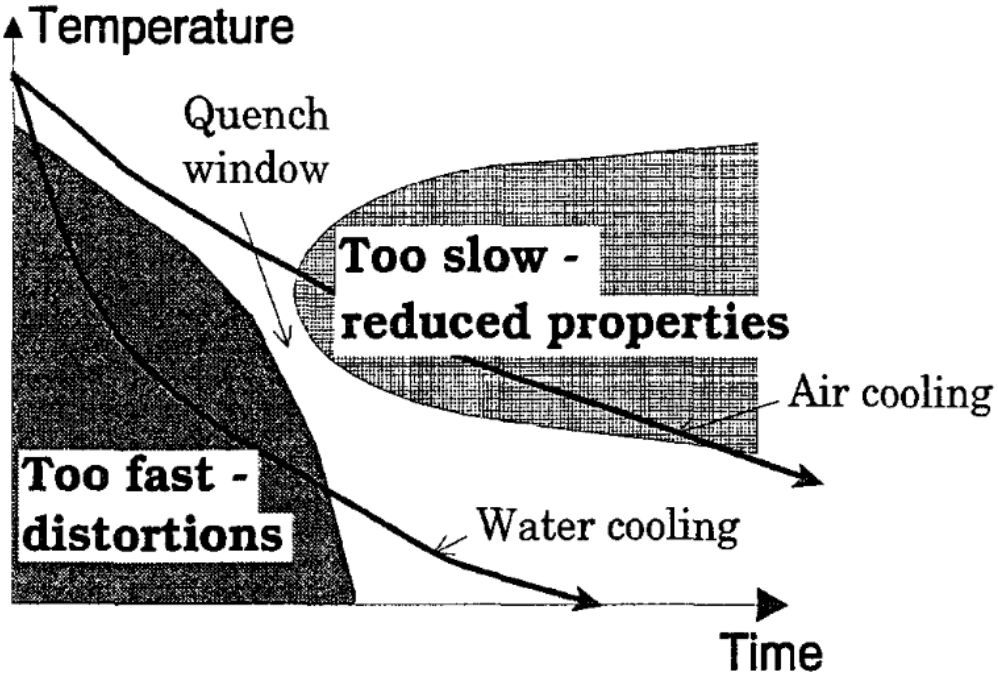

Figure 1.5.5: The window for quenching of aluminium (Jarvstrat and Tjotta n.d.)

as an already done test has gotten. If that is the case, this will give some good validation to the simulation, where it then will have to be validated in the other direction by taking a new profile and running this in software first before running the extrude and quenching with the same settings and measuring if the results match, but this part is outside the scope of this thesis, as it will only look at the first step of reproducing the already done test to see if the results are the same. Another thing that is outside the scope of the thesis is a lack of data on distortions of the profile both from the extrusion and quenching.

CHAPTER

TWO

THEORY

Extrusion involves reshaping a material by applying pressure to force it through a shaped opening, causing the atoms to slide past one another and form new bonds, resulting in the desired shape of the extruded product. (Chahare and Inamdar 2016)

2.1 The Extrusion Process

Before the extrusion can begin, a few things need to be done both to the material being extruded and to the extrusion press and its components and tools. One of the most important ones for aluminium is bringing the material to temperature. At room temperature, aluminium is too solid and hard with the difficulty that it work-hardens when deformed, making it even harder and more brittle. This problem is fixed by heating the aluminium to a temperature not far below its lowest melting temperature for the alloy used. When metal is at or close to its melting point, it has the lowest viscosity and the easiest to deform plastically. However, being this close to melting also makes it incredibly sensitive, where too much heat will start melting the material. For this reason, the material is kept at a lower temperature because if it melts, the alloy is, in the best case, weakened and,

worst case, useless. Also, there are higher chances for imperfections and faults when working close to the redline. (Saha 2000)

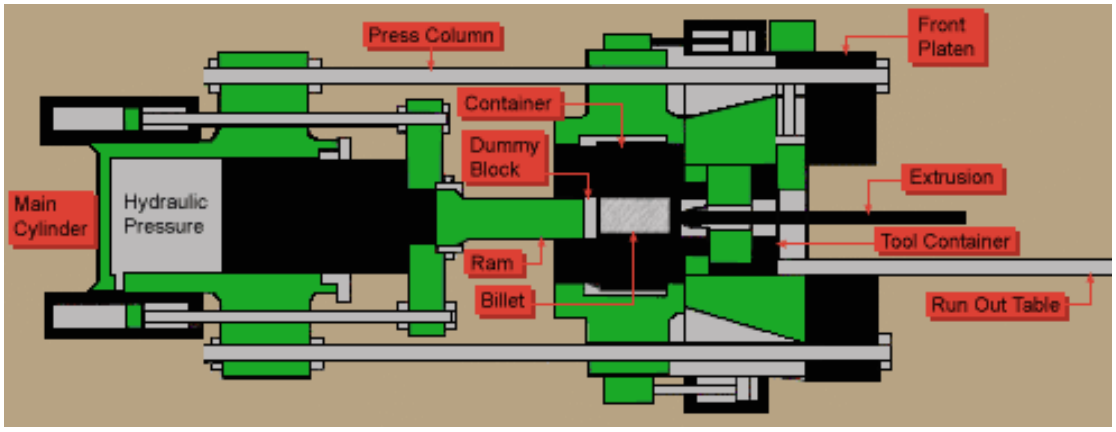

Figure 2.1.1: Diagram of the different parts in an extrusion press. (*ALUMINUM EXTRUSION PROCESS* 2022)

To prevent the aluminium from cooling too quickly, it is necessary to heat the parts of the extrusion press that come into contact with the material and the features that are in close contact with those components. Some cooling is required to keep the aluminium from reaching melting temperatures from the heat generated during the extrusion process. Still, it has to be controlled and limited compared to putting 400 °C aluminium in direct contact with room temperature steel. This contact will cause rapid cooling of the outermost aluminium. At the same time, the inner material stays at a higher temperature, giving large gradients and a highly inconsistent material to extrude. (Flitta and Sheppard 2013a)

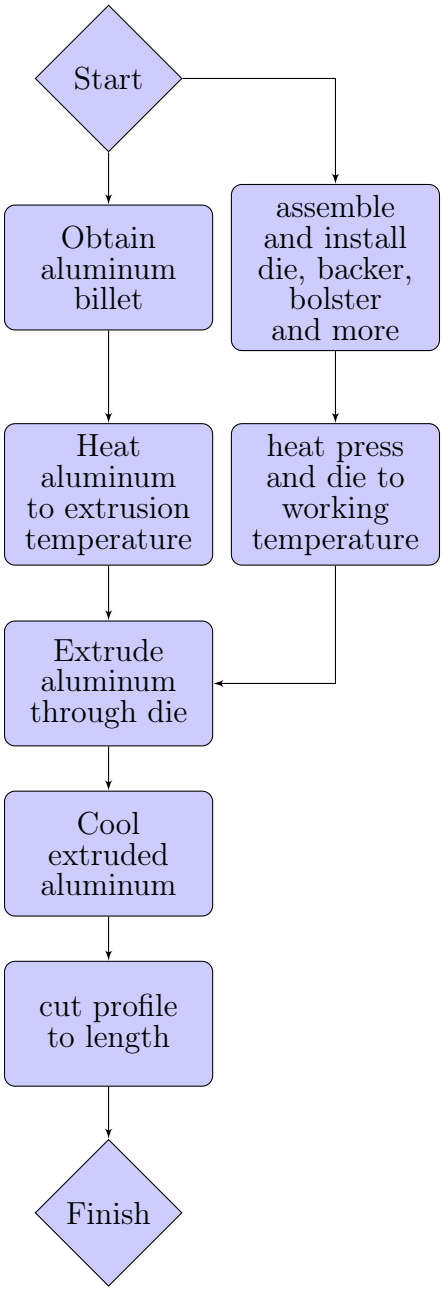

Figure 2.1.2: Flowchart of how an extrusion process flows

2.2 The Cooling Process

When working with an extrusion, the product coming out of the press is at many hundreds of °Cs hot and needs to be cooled down, which usually needs to happen quickly too. The simplest way of doing this is by letting the beams passively cool in the air, which takes a long time and decreases the risk of extrusion warping but can sag under its weight, and it also does not give any good quenching. So to fix these problems and make a faster cooling process, there is the cooling box, a

long box filled with nozzles spraying water or air at the beams as they come out of the press. The water or air streams will then rapidly cool the profile to a more stable temperature closer to room temperature. This cooling is usually done with a puller pulling the beam to ensure it stays straight. There is also the option of varying the pressure on the different nozzle rows to more or less gently push the profile in different directions to keep it straight and keep it from warping while it is cooling down.

2.3 Parameters Affecting The Extrusion Process

Extrusion is the most straightforward method of making beams with a consistent cross-section. The material starts as a massive cylinder and is heated to make it malleable enough to be formed by pressing it through a form. Although the real world is not simple, many more things must be considered. It is still metal, even if heated too close to being a liquid. It will need considerable forces in the range of 20-30 MN depending on the billet's size, the extrusion ratio and the complexity of the die it is being forced past. This pressure gives high stresses and strains both in the billet itself as it is getting plastically deformed and in the die, backer and other parts of the press as they get pushed outwards by the billet. Other places of large strains are around dead metal zones and the die during extrusion when the material flows down into and through the die. From here on outward, for this thesis, this thesis will mainly focus on direct extrusion. Most of this will apply generally but needs to be confirmed before being used in anything critical.

The extrusion parameters that will be used in this thesis are as in table 2.3.1:

Table 2.3.1: Extrusion temperature and geometric parameters

	Temperature [°C]	Length [mm]	Diameter [mm]	HTC $[W/(m^2 * K)]$
Billet	450	1000	280	
Taper	50			
Die	460	161	400	
Container	400	>1000	288	
Dummy block	400			
Case	460		400	5000
Pressure ring	460		250	5000

2.3.1 Friction

One of the most influential parameters is friction, which comes from the walls and surfaces where the material slides past and between the material itself as it deforms and slides along during the extrusion process. Look at the friction from the ram/dummy block pushing the material. The first and simplest friction meet is the friction between the container walls and the material. This friction creates heat and holds the material closest to the wall. This friction can hold back the impurities along the outer walls of the billet, creating a purer extruded profile. Something making this phenomenon possible is the high friction and low shear strength of the material in these high temperature and pressure conditions. It gives a phenomenon called sticking friction, where friction equals the material's shear strength, making it stick to the surface and shear off instead of getting pushed along with the rest of the material. Next in line is the friction on the top of the die holding back the front end of the billet, keeping the impure material out and making what is called a dead zone of material around the corner of the container and die interface. This dead zone gives rise to the first material-to-material slip plane and friction. As this is a complex thermal, mechanical and thermomechanical environment with high pressures and temperatures, coefficients like the frictional

coefficient are not as simple as a constant variable. When the material is as hot as in an extrusion process that usually happens to be not too far below the melting point of a specific alloy, the friction coefficient also depends on the temperature in the specific area. Another thing making this step more complicated is the high deformation and plastic strain rate happening to the metal, especially around and in the die. (Flitta and Sheppard 2013b)

2.3.2 Temperature

Temperature is one of the most important parameters and symptoms to control when extruded aluminium. The main job of doing aluminium extrusion at a higher temperature is reducing the forces needed to get the aluminium to deform and flow through the die. This force reduction comes from the aluminium having a yield strength of a few hundred MPa at room temperature to only having a few tens of MPa at extrusion temperatures in the 400°C plus range. The heating of the billets is typically done in either a gas furnace or with induction heating. The billet is then kept at temperature to get a homogeneous temperature gradient through the whole billet before it is taken out. It is either given a temperature taper (hot end towards the die) or put directly into the extrusion press. Giving a temperature gradient is the most used method as it gives a more steady exit/operating temperature on the aluminium and makes it easier for the air to get out of the extrusion chamber when adding a new billet. (Saha 2000)

Temperature is also important for the extrusion press and all its parts, especially those in close contact with the hot aluminium. Due to the high operating temperatures of the extrusion process, the metals used in it will generally have different characteristics compared to when at room temperature. These steels must keep these characteristics within the operating temperature parameters where the metal is strongest and toughest to prevent deformation or cracking from normal use. The lifetime of the steels used in the mandrel can vary greatly depending on the temperature at which they are operated. For example, if kept below 450 °C, the lifetime of the steel may be 10-15 years. However, if the steel is continuously or frequently operated at 500 °C, it may significantly reduce its lifetime to only 1-1.5 years.

Special high-temperature steels may require heating up to 380 °C to reach their toughest state and ensure crack-free operation. (Hähnel, Gillmeister, and Kräger 2016)

2.3.3 Extrusion Pressure

Extrusion pressure is applied to the billet by the ram and inside the billet. The most accessible pressure to figure out is the pressure applied to the billet by the ram, which is a simple force divided by area calculations. The pressures in the rest of the billet are harder to figure out as they will decrease from having to overwin the opposing forces from friction against the walls and the shear forces inside the material, whichever is the strongest in each place. This friction means the pressures will drop further away from the ram one is looking at. And especially for port-hole dies where there is a need for relatively high pressures in the welding chambers to secure good weld quality. This can cause some problems with ensuring the forces are below the limits of the specific press used.

As shown in figure2.3.1 below, different pressures are needed for the different extrusion types. The first part of the graph is the initiation stage, where the billet is just loaded into the camber, and the ram has started pushing. Still, as the billet is a little smaller than the container, the billet needs to fill the whole volume before any significant forces develop. The next stage is the hump with the peak pressures/forces. This part is where the billet fills the die and settles into its steady state for the extrusion cycle. Steady-state is a bit different for the different extrusion types since direct extrusion has to overcome the friction forces against the container walls, which the others do not have. The slight difference between hydrostatic and direct is explained by hydrostatic having even less friction as fluids surround the billet. Usually, some oil-based fluid lowers the friction. Lastly is the increase in pressures for the direct and indirect extrusions where the butt-end of the billet is formed and is started compacted. This point is also usually the point where the cycle is stopped to keep the impurities from getting pushed into the die and extruded profile.

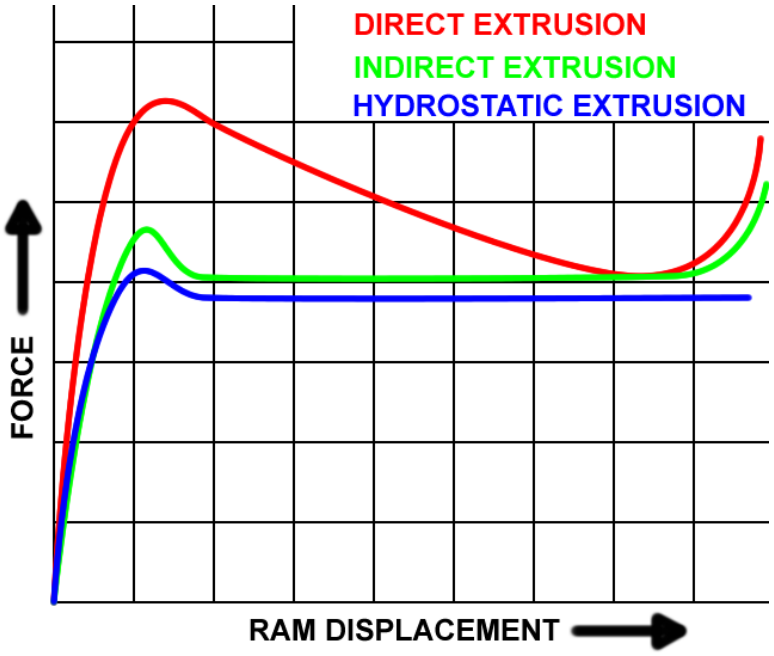

Figure 2.3.1: The pressure/displacement profile for the different extrusion methods (*File:Extrusion force plot.png - Wikimedia Commons* n.d.)

2.3.4 Extrusion Ratio

The extrusion ratio is the ratio between the billet's and profile's areas after being extruded (see figure2.3.2). This number is also a good indicator of how much the material has to change during the extrusion process, as a large extrusion ratio will give a significant change in size. This change leads to a lot of material flow in and around the die, again causing a lot of friction, turbulence, and heat to be generated with the significant difference in the area. it is one of the most important contributors to the exit temperature during the extrusion process, especially at higher ram speeds (Abdul-Jawwad and Bashir 2011).

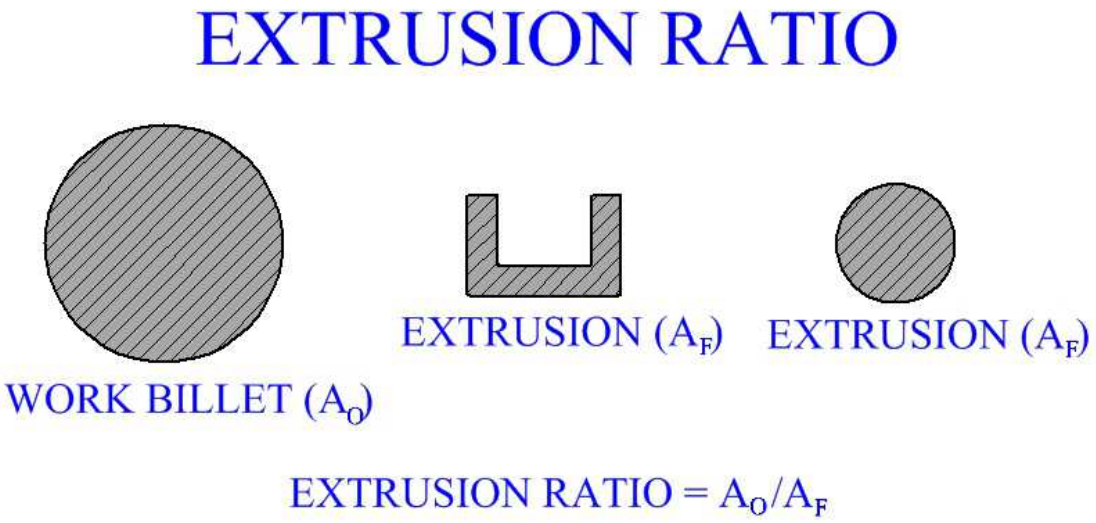

Figure 2.3.2: Extrution ratio (*the library of manufacturing, extrusion* 2022)

The extrusion ratio also influences other profile characteristics, like how the grain structure is affected during the extrusion process. This metallurgical change is a reason for the rule of thumb that the extrusion ratio should be over 10:1 to ensure enough mechanical work is performed on all of the material to give suitable mechanical properties. There is also a soft maximum limit of 100:1 for mild to medium alloys before it gets too difficult to press the material through the die. For hard alloys, the ratio is 35:1 before the pressure needed to push the material gets too high and gives a too-high temperature from the deformations and extra work being done to the material. There is a significant effect on the shear angle between the dead metal zone in front of the die and the extrusion ratio. A larger ratio will give a larger angle from the extrusion direction, while a smaller ratio will give a smaller angle. (Saha 2000)

2.3.5 Ram Speed

The ram speed is the parameter with the most self-explaining name and the easiest to control during operation. As the ram speed is the parameter that changes how fast things happen. It also works like the scaling factor between the parameters that do change based on the speed, like the flow stress, the work being done per unit of time, the flow turbulence and those that do not change with the flow speed, like the heat transfer, extrusion ratio, die geometry and friction coefficient

as examples (Abdul-Jawwad and Bashir 2011). This means it is one of the most effective ways of regulating the exit temperature in production to lower the ram speed. This slower ram speed lowers heat generation from effects like flow stress, friction, and redundant work. While the thermal transfer stays the same, giving the material more time to cool. On the other hand, time is money, and to keep the productivity of an extrusion press up. The rem speed must stay as high as possible while keeping temperatures under critical values for the specific alloy. The parameter with the highest correlations with extrusion pressure with an almost linear function between the ram speed and the pressure reported by the press. (Saha 2000)

2.3.6 Billet Lenght

Another parameter that should be maximized in most cases is the length of the billet, as the longer the billet is, the less stopping needs to happen, which in turn gives higher productivity and less waste. This fact comes from the more volume in the billet, the longer the steady-state extrusion, giving longer extrudates with pristine quality and fewer stops where the butt-end has to be cut off, and fewer transition welds need to be cut off. Sadly it is not as simple as just making the billet longer, as there are many limiting factors, among them are the maximum force of the press, the length of the run-off table and the length of the container. The maximum force of the press is limiting because the increased frictional forces with longer billets when doing direct extrusion will, at some point, get higher than the press can handle. And there is also the length of the run-off table to consider, as that is a hard stop for the extruded profile since the puller is needed to keep the beam straight, especially as it gets longer and encounters more friction. So the optimal length of a billet is to match the useful aluminium volume of a billet to the volume of the full-length profile that can be extruded at the current facility. (Saha 2000)

2.3.7 Die Geometry

The die is what, in the end, determines the cross-section of the extruded beam. Depending on how it is counted, there are two main types of dies. There are

flat dies, which are simpler dies which are a single flat disc with either just the bearings for the profile or some holes over the profiles to equalize the flow of material into different parts of the bearing. The other type of die is a port hole die (see figure2.3.3), usually made from two or more metal discs, where the lower part of the die parts is somewhat similar to a flat die but with a giant hole(s). This part of the die is the yellow section of the die in figure2.3.3. The other disc(s) have larger trough holes with a mandrel in the middle to give finished profiles with one or more holes. (Qamar, Pervez, and Chekotu 2018)

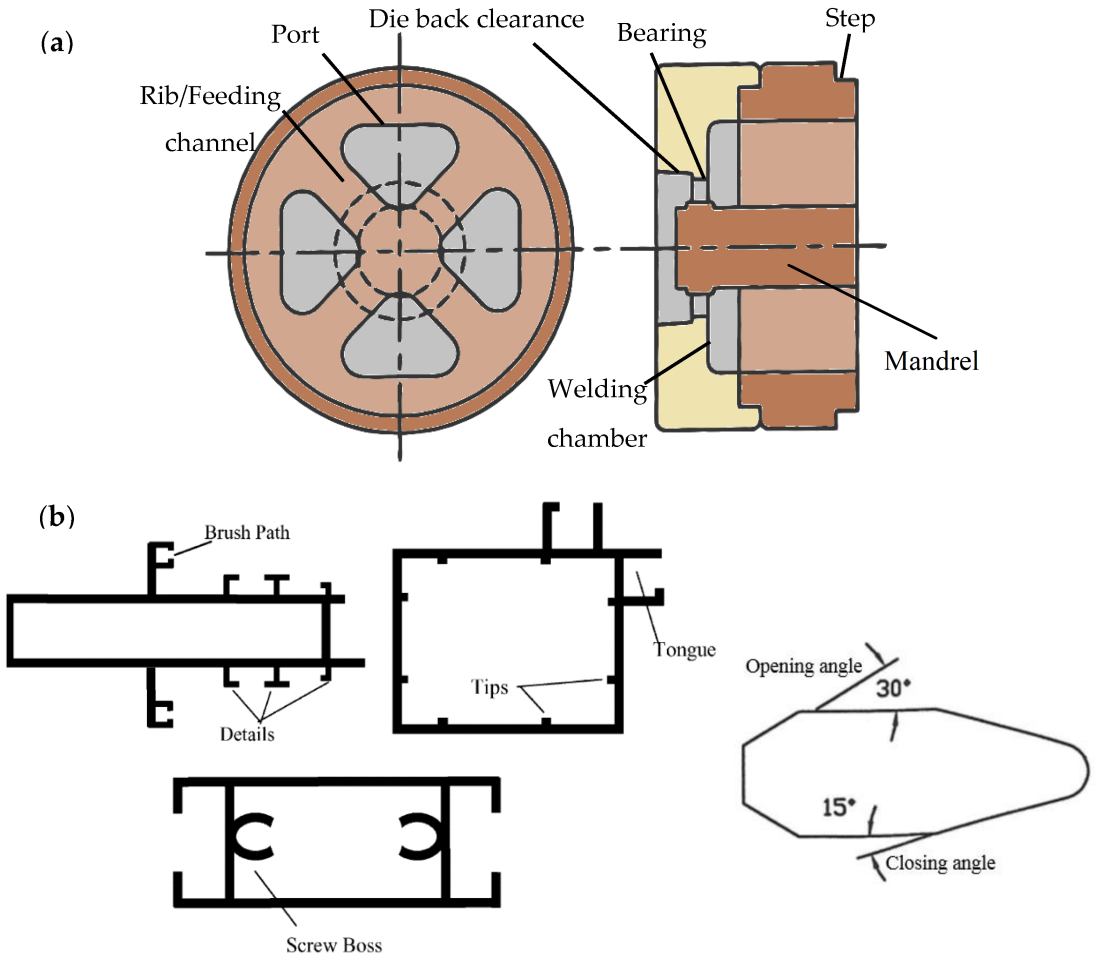

Figure 2.3.3: (a) Main features on a port-hole die (b) some typical features on extruded profiles (left) and details of a die rib profile (right) (Qamar, Pervez, and Chekotu 2018)

Pocket dies are more versatile than flat dies, but this comes at the cost of being both more expensive to produce from the fact of being more parts with more

complicated geometry. This complication makes them harder to design, both from being more parts, but now there are welding zones that must be thought about and considered. These welding zones come from the bridges holding the mandrel, forcing the material to flow around them. When the material has gotten around the bridges, it has to be welded back together properly before passing by the bearings to avoid streaks or missing material in the finished profile.

The first noticeable features of a die from the extrusion side are the inlet ports for a mandril die and the pockets for a flat-face die. These openings decide how much material goes into each die part and how easily the material flows. Various factors accomplish this. Among these are the simple stuff, the size of the hole and how easily the material flows down through it. Other factors like the distance from the centre, the slopes and geometry of the opening and how the friction between everything influences the material as it flows into the hole and through the die. (Saha 2000)

Next in line into the die are the welding chambers, where the metal streams meet and get welded together. This welding process is similar to forge welding in that two or more metal streams meet at high temperatures and pressure and get "forged" together into a single piece of metal before being forced into the bearings.

The part of a die doing the final shaping of the material as it exits the die is called the bearings. The bearings have two main tasks in the extrusion process. The first of these jobs is doing the final forming of the material as it flows past. This position makes them the most important part of getting the right size and shape. There may be a way of adding some extra material to compensate for the deflections of the die material during extrusion, for example, the bearing being a bit smaller than they had been if infinitely stiff so that they deflect outwards during extrusion to the correct size while extruding. The other job is fine-tuning the friction forces in the different areas to fine-tune the exit velocity of the different parts of the extruded cross-section and keeping the pressure in the welding chambers to facilitate good welding quality. (Saha 2000)

Lastly is the relief area of the die, called "die back clearance" the figure2.3.3. This

is there to support the bearings and the rest of the die. This does not require fancy geometry, so it is, for the most part, just a hole a few mm larger than the bearings and a flat bottom surface for it to transfer the forces into the backer (see figure2.3.4) that then transmits then further onto the bolster and sub-bolster (if used) and lastly onto the power ring (dark grey in figure2.3.4) and lastly onto the press plate.

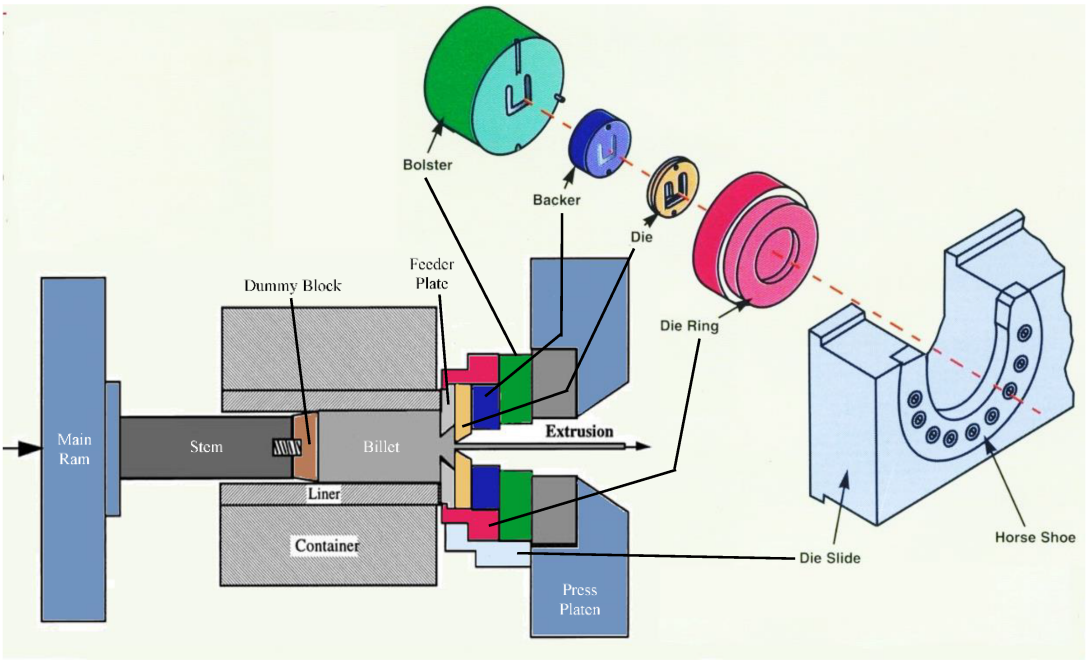

Figure 2.3.4: Diagram showing different parts of the die in a press (*ALUMINUM EXTRUSION PROCESS* 2022)

2.4 Parameters Affecting the Cooling Process

When quenching, The controllable parameters are not as plentiful as it is for the extrusion process itself. The profile speed is set from the extrusion, so it is all about doing the quenching as it passes through. As for controllable parameters, there are the type and placement of nozzles and how much fluid is pushed through those nozzles.

2.4.1 Temperature

The primary decider for heat transfer is the temperature difference between the cooling fluid and the material being cooled, and this comes just from the formula for heat transfer:

$$\dot{Q} = k * A * dT \tag{2.1}$$

Where $\dot{Q}$ is the amount of heat in Watt that is being transferred, the k is the coefficient for how fast this transfer goes, and the dT is the difference in temperature between the fluid used for cooling and the material being cooled. This then gives us that all else being static, the higher the difference between the fluid and the material, the more heat we can remove from the material. This works in our favour as the aluminium is in the range of 400-600 °C when it comes out of the extrusion process. The water that is, in most cases, used for cooling has a boiling point of 100 degrees C, so this is the max temperature the water can be, but it is usually kept at a reasonable 20-50 °C. for it to be safer to be around and also is more effective at cooling. (Hall et al. 1997)

Though it is not this simple, because of the high difference in temperature, the water will rapidly boil when hitting the hot aluminium. This effect is called the Leithenfrost effect, which is the effect of water creating a steam/vapour layer between the fluid water and the hot surface, acting as an insulating barrier between the fluid and the aluminium. This happens at temperatures above 300 °C. As this boiling takes energy, there is still cooling, but it is lower than when there is full fluid contact with the surface. The lowest cooling point is the lowest temperature where the Leithenfrost effect is effective. At higher temperatures, the boiling happens faster, consuming more energy and at lower temperatures, there is more surface wetting, giving fluid contact and higher heat transfer. (Xu et al. 2014)

In between single-phase cooling, as described first, and the Leithenfrost cooling temperatures is where there is the highest cooling where the surface is thoroughly wetted. The water is rapidly boiling and transporting away the heat as steam.

This happens in the range between 170 and 300 °C. (Xu et al. 2014)

2.4.2 Profile Geometry

The thickness of both the profile and the walls will have a lot to say on the cooling performance and especially the homogeneity of the cooling. This comes from the heat transfer inside the material being limited to the intrinsic heat transfer coefficient of the base material and the lag in transfer because of the temperature gradients. Depending on the temperature of the aluminium, the heat transfer to the water can reach the $15 - 20kW/m^2 \cdot K$ range. In contrast, the heat transfer inside the aluminium is $238W/m \cdot K$ for pure aluminium and is lower when alloyed (with higher alloy content giving lower heat transfer). This discrepancy in heat transfer and the fact that there needs to be a temperature gradient to get heat transfer. This takes time to propagate through the material, resulting in uneven cooling and worsening the thicker it is. (Xu et al. 2014)

The geometry itself does also play a role. When there is a structure in the middle of a profile, this material will not get sprayed by water and is then not cooled other than the internal conductive heat transfer giving the same effect as a thicker wall thickness. In this case, there is less material to conduct, slowing the heat transfer even further.

2.4.3 Water Flux

For faster cooling, more water flux is better, with diminishing returns. As more mass of water gets sprayed onto the aluminium at a higher rate, there will be a larger amount of colder mass for the heat to be transferred to, but as this transfer has its limits, there will be diminishing returns. There is also the effect of trying to force more water onto the surface, increasing the pressure on the surface, trapping bobbles of air and steam on the surface, where they act as insulators, further limiting the return in increasing the water flux. (Xu et al. 2014)

2.4.4 Water Surface

Given water's different behaviours at different temperatures, there will be differences in how and how much heat it conducts at different temperatures. Starting at the most mundane conduction cooling from aluminium to water in one phase, cooling gives linear scaling with a temperature delta between aluminium and the water. When the aluminium gets over 100 °C, the water starts to boil, giving a much higher heat transfer, which is still mostly linear until the aluminium gets hot enough that the water boils before it covers the surface fully. The highest heat flux coefficient is before the water cannot cover the surface. At even higher temperatures, the water is in the transition boiling regime, where the surface is somewhat covered in water and quickly boils off. At even higher temperatures, the leidenfrost point is reached where the water does not reach the surface before boiling, giving the lowest heat flux. Over this temperature, the boiling happens even faster, giving a higher HTC and fully into the film boiling regime. (Hall et al. 1997) (Deiters and Mudawar 1989)

2.4.5 Profile Surface

In the boiling regime of cooling in the 170 to 300 °C range, the roughness of the surface does have some impact on the heat transfer coefficient of the aluminium to the water. In tests, it is shown that a smooth surface Ra = 0.6 µm does get a higher maximum heat transfer than a Ra of 7.6, and the highest is at a rougher surface with a Ra of 40.2 µm giving the highest heat transfer. But these differences are only taking effect when getting below 200 °C, where there is complete wetting of the surface. The smooth and rough surfaces are practically even down to about 130 °C. At higher temperatures, the Leithenfrost effect makes a vapour layer thicker than the surface's unevenness, diminishing the effect of the different surface finishes. (Xu et al. 2014)

CHAPTER

THREE

METHODS

This thesis will compare the force and exit temperature results between an extrusion and a simulation, the temperature data gathered during a quench box test, and a simulation done of the same quench box test. This is done to try and validate the simulations done in QForm. The goal of simulations is to give the industry cheaper ways of testing and optimizing new processes. In this case, the process of making dies for extrusion and quenching the extruded profiles. This thesis aims to indicate how good the simulation software QForm is and how well it can be used in the industry for the abovementioned purpose.

3.1 Extrusion Process and Experiments

Industrial extrusion and cooling experiments were conducted at Benteler Automotive Raufoss to produce the profile shown in figure 3.1.2. As this is a profile with holes in the middle, the die must have structures both in the middle of the bearing and above it to keep it in place. This leads to a two (or more) part die as seen in figure 3.1.1 where both the lower part has the outer perimeter and half the welding chambers of the die. At the same time, the upper part has the middle structure of the bearing plus the support structure and the pockets funnelling the

aluminium in the right proportions to the different parts of the bearings.

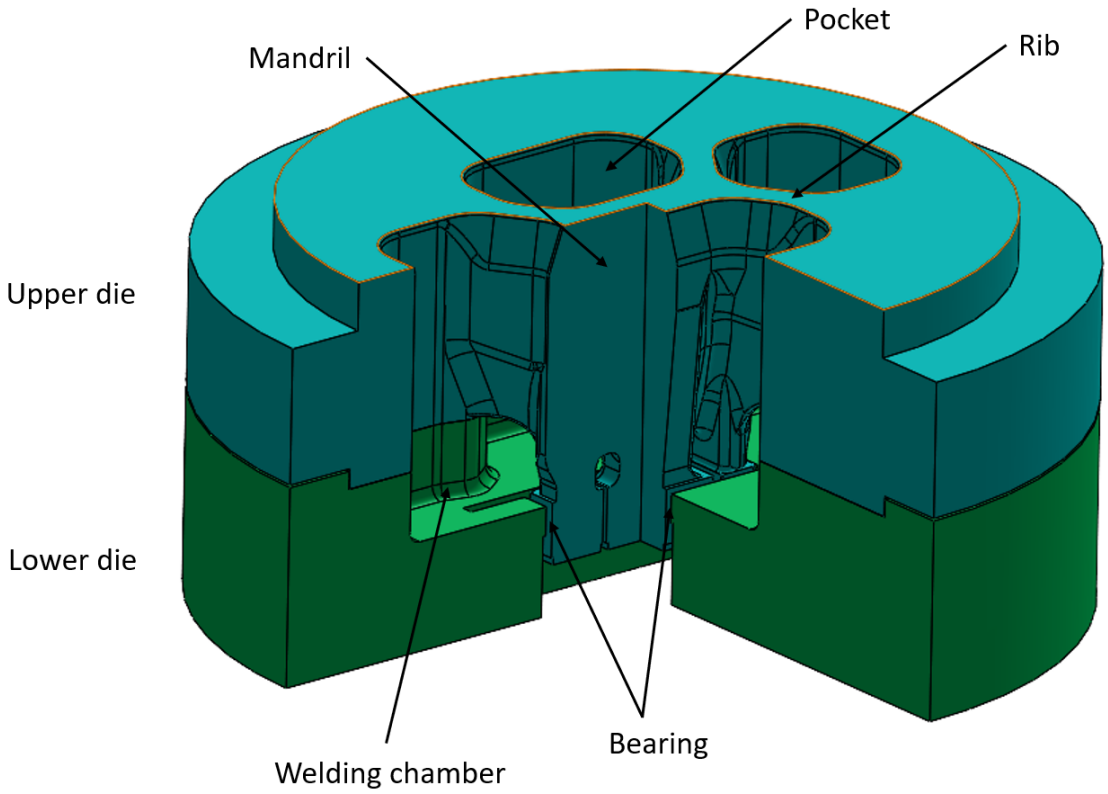

Figure 3.1.1: Die with cutout

For these comparisons between test results obtained from Benteler and the simulation results obtained from the simulation software QForm, the profile test is shown in figure 3.1.2. This test profile is made to have a little bit of everything, like thick and thin protrudes, different wall thicknesses and changing wall thicknesses.

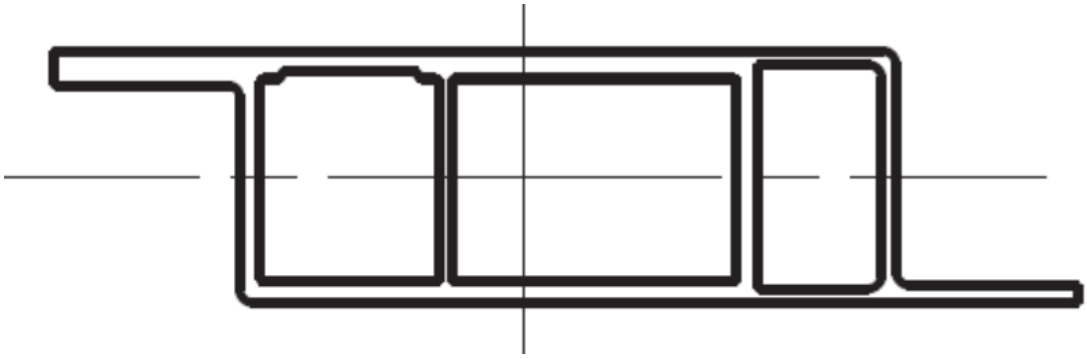

Figure 3.1.2: Test profile from Benteler

The extrusion process started with a 280Ø x 1000 mm billet of 6005 aluminium alloy. This profile is heated before being put into the extrusion press container.

Where it is pressed past a porthole die to get the right shape. When the profile has gotten out of the extrusion press, a temperature measuring device is placed on top of the profile to measure the temperature of the profile as it passes through the quenching station. The temperature measuring unit, as seen in figure 3.1.3, is a unit made by Hydro for measuring the temperature of extruded profiles as they go through the quenching box. The two probes that do the measuring stick out on the figure's left side. The temperature is then measured and stored inside a computer inside the large aluminium box. The datalogger box is standing on four sharpened legs, and with the weight of the logger, it is heavy and stable enough to stay in place when going through the cooling station, even during a standing wave test.

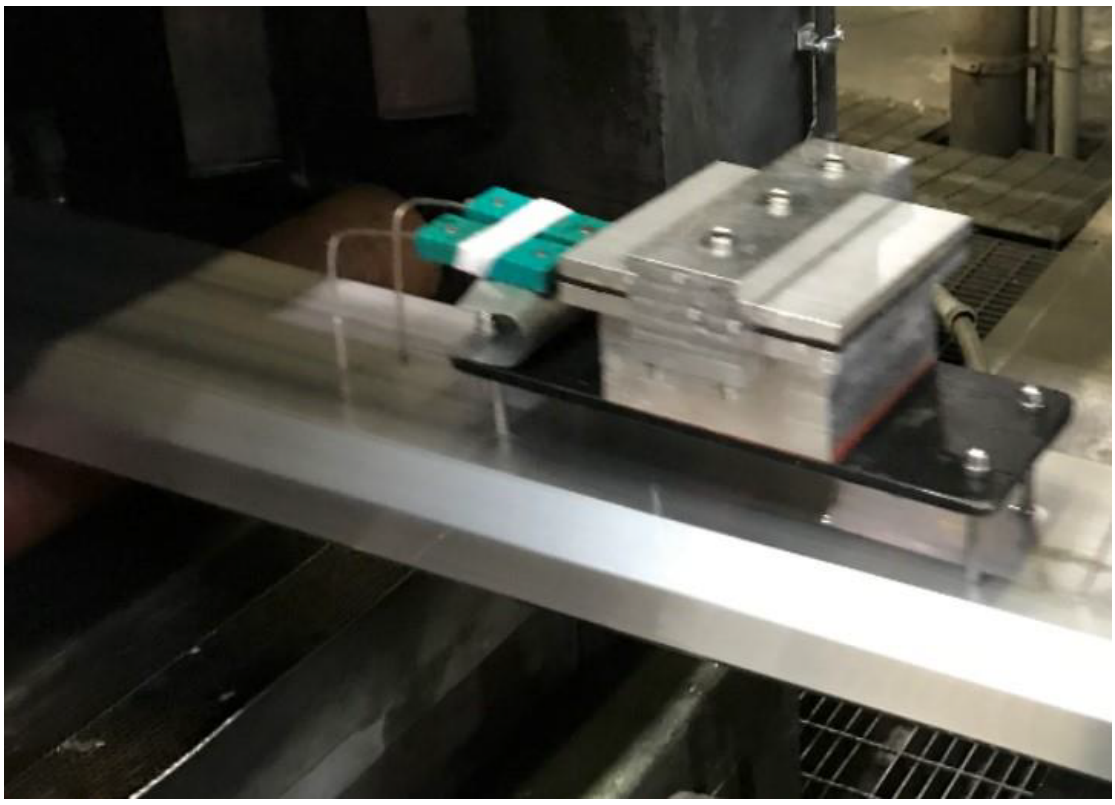

Figure 3.1.3: Temperature measuring unit made by Hydro

3.1.1 Materials

The material being used in the test is the aluminium alloy 6005. For the simulation, the extrusion version of the 6005 alloys is used as the closest material supplied by the program. Below are the material parameters and equations that are being

used by QForm when doing the simulations. There are three different ones, where a comparison is made in chapter 4.2.1, between these and the higher accuracy simulation mode specifically for temperature in QForm with the QForm material parameters.

The material parameters for flow stress are provided together with QForm for 6005 using the formula:

$$\sigma = A \cdot e^{m_1 T} \cdot T^{m_9} \cdot \varepsilon^{m_2} \cdot e^{m_4/\varepsilon} \cdot (1+\varepsilon)^{m_5 T} \cdot e^{m_7 \varepsilon} \cdot \dot{\varepsilon}^{m_3} \cdot \dot{\varepsilon}^{m_8 T} \tag{3.1}$$

In equation 3.1, the σ is the true stress in MPa, T is for temperature, ε is the true strain during deformation, $\dot{\varepsilon}$ is the true strain rate during deformation, and m_x are the parameters for the behaviour of each material. Using at least 6 of these is recommended by the ICEB (Llorca-Schenk, Rico-Juan, and Sanchez-Lozano 2023).

With the parameters in table 3.1.1 added:

Table 3.1.1: Values QForm uses for its 6005 extrusion material

Symbol	A[MPa]	m1	m2	m3	m4	m5	m7	m8	m9
Value	320	-0.00511	-0.12422	0.1	-0.01364	0.00024	0	0	0

Next are the literature (Pinter and Mehtedi 2012) and Benteler-provided materials:

$$\sigma = \frac{1}{\alpha} \sinh^{-1} \left[\left[\frac{1}{A} \cdot \dot{\varepsilon} \cdot exp\left(\frac{Q}{RT_{abs}} \right) \right]^{\frac{1}{n}} \right] \tag{3.2}$$

In equation 3.2 does the symbol σ mean the flow stress in MPa, α stands for the reciprocal stress factor in 1/MPa, A is the reciprocal strain rate factor in 1/s, $\dot{\varepsilon}$ is the effective strain rate in 1/s, Q is the activation energy in J/mol, R is the universal gas constant, T is the temperature, and n is stress exponent. Of note is that the material parameters given by Benteler lack detailed information about how they were produced and have ambiguity around the quality of the material parameters.

Where the values in table 3.1.2

Table 3.1.2: Benteler and literature parameters

Symbols	**L**iterature values	**B**enteler values
A [1/s]	9.84e9	7.55454e10
Q [J/mol]	182798	164800
n	5.16	3.649
α [1/MPa]	0.053	0.0396

3.1.2 The Quensh box

The quench box is a cooling box made by Presezzi Extrusion from Italy. It is set up with four different zones for cooling where each can be controlled individually, but for these tests, the first three are combined into one zone, giving two equal zones to control to simplify the testing. This gives two zones controlled between 10, 50 and 100%. There is also the option of using a standing wave in the quench box, where the box is filled with standing water held in by the pressure of the nozzles at the end of the quench box.

For the nozzles, there are in the bottom two lines of 18 sets of 4 nozzles, where the two outer ones are the GYU 1581 nozzles (large nozzle) with a 90°spread angle, and the inner nozzles are the GYU 1310 nozzles (small nozzle) in each set. For the sides, there are 36 sets of 2 nozzles on each side. Where the upper nozzle is the smaller one and the lower nozzle is the larger type. Lastly, there are two lines of 36 sets of two nozzles for the top, with the outer being the larger and the inner being the smaller variant. This setup is shown in figure 3.1.4, where the profile is extruded from the bottom left to the top right.

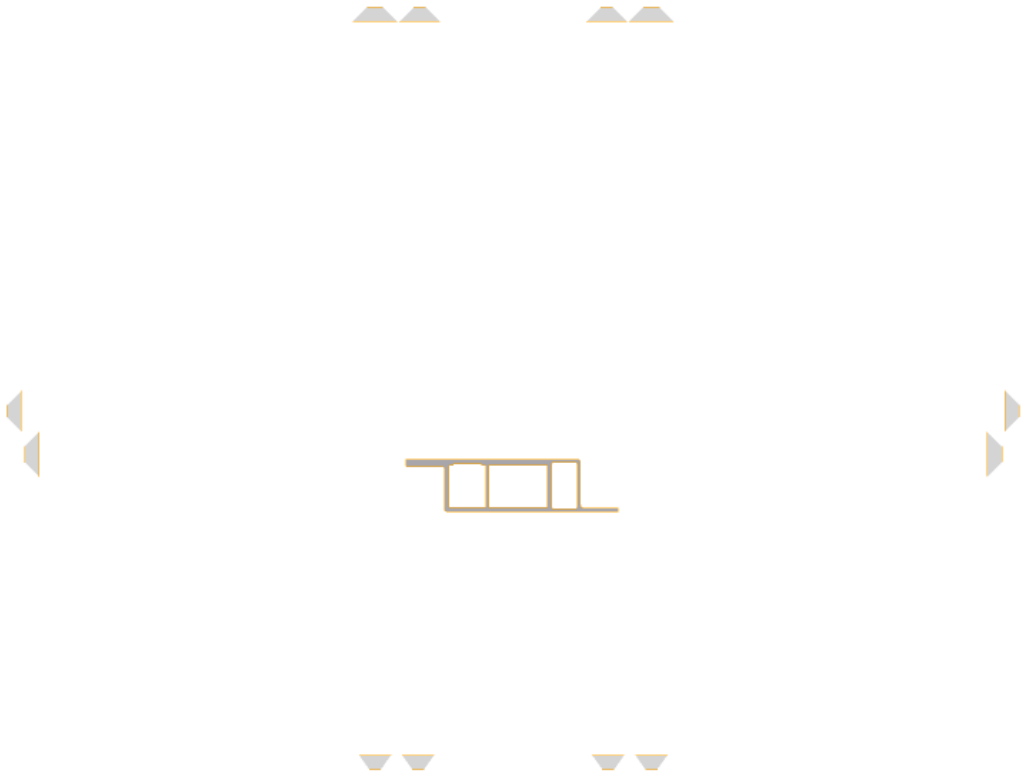

Figure 3.1.4: Figure showing how the nozzles are set up in the simulation

We need to figure out the set-up as closely as possible to do cooling simulations as close to the quench box as possible. We are starting with the nozzles and their water flux. From the BOM and drawings, we find 210 of each nozzle. This, together with the maximum use of 84 litres per minute for the smaller nozzles and 94 L/min for the larger ones. Dividing this out gives 0.410 L/min and 0.448 L/min for the smaller and larger nozzles, respectively.

3.2 Numerical Modelling of Extrusion and Cooling Processes

For the numerical modelling, the program QForm 10.2.1 is used. QForm is a simulation software specifically made to model plastic metal working and quenching of those formed metal parts to give a good tool for simulation work on hot metal before starting testing and forming in real life. For this thesis, the module for extrusion and cooling of extruded profiles is the most interesting.

3.2.1 Extrusion simulation

In QForm, there is also the integrated software called QShape which is a program to take in different 3D model files, preferably STEP files, to do the process of meshing the die, defining the bearings, assessing where the metal will flow and building up the stack of the die, backer, bolsters and sub-bolster. They are also meshed and made ready to be used for simulation. The finished product from QShape will look like in figure 3.2.1, where the blue is the dummy block, the red is the billet, the turquoise is the upper die, the green is the lower die, and the purple is the bolster. Then when back in QForm, the following steps define all the variable parameters that are not geometry dependent, like the temperature of different parts, the extrusion speed, the materials the die and billet are made out of and the simulation settings. The material characteristics for the billet and the die are all user definable. New material parameters can be added if the included materials are not what you need. As can be seen in some of the results from the study (Medvedev et al. 2020), where they compared their tests, a material they input from data gathered and included material from QForm. The included materials are imperfect, so some caution may be had while using them, and better results can be obtained by getting the necessary data. However, the materials are not too far of and are made conservatively, giving slightly higher numbers in simulation compared to the real world.

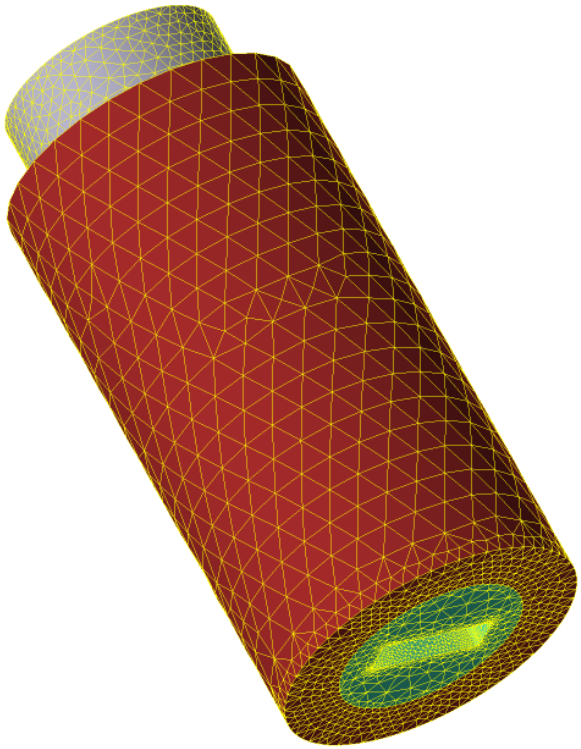

Figure 3.2.1: Figure of the billet, die and bolster before simulation

The added temperatures are in table 2.3.1. Further is the temperature of the die-set, which is the turquoise and light blue parts in figure 3.2.2, where below is the bolster in purple. Then it sets the container and dummy block temperatures, the dark blue and yellow parts. Lastly, the casing and the power ring are the red sides and the ring at the bottom is seen in figure 3.2.1. They also have a fixed HTC that is set.

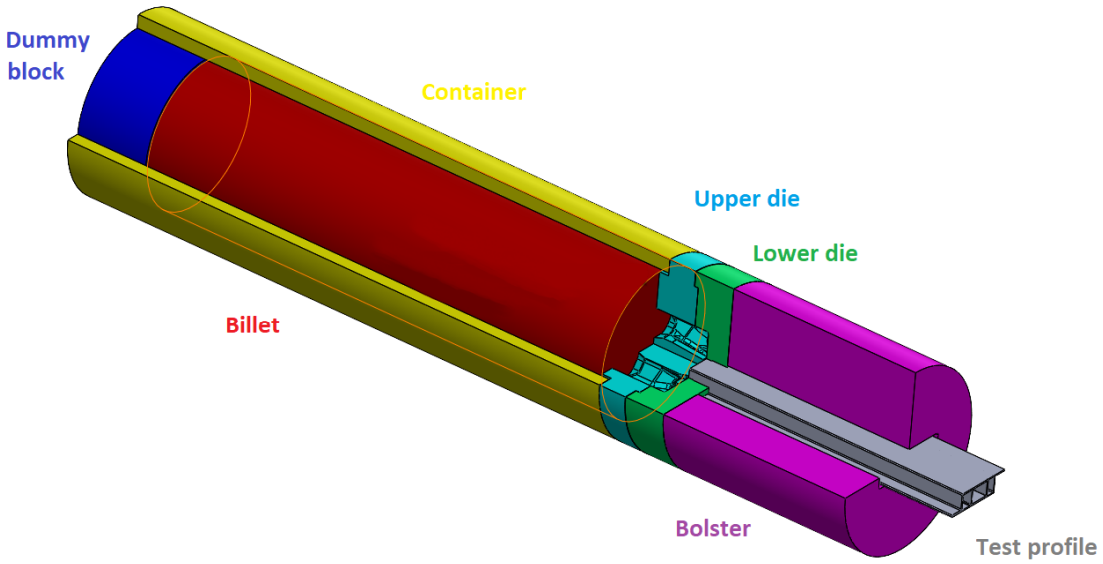

Figure 3.2.2: Cross section of dummy block, container, billet, die, bolster and profile

3.2.2 Cooling simulation

For the cooling simulation, there are two options for the input of profiles. This is either a simple drawing in a DFX format or an export from the extrusion in the csv2d format. When using the simple DXF format, the temperature and stress in the profile have to be added as parameters, and there is only possible to get a homogenous distribution so there are no gradients. In the case of the csv2d format, these data are brought over from the extrusion simulations that give the profile temperature and stress gradient fields.

From here, the csv2d file is imported from the extrusion simulation. This gives the temperature and stress field from the extrusion simulation. This also selects the material being used. During the temperature simulation in the quench box, the profile is moved at a distance of 10 mm each step, but this is an adaptive number, so in run time that number will be lower. The profile velocity is set at 19.5 m/min. The stop condition is set to 31 seconds, giving enough time for the profile to pass through the whole quench box. The nozzles are set up like in figure 3.1.4 and described in section 3.1.2.

Using the numbers in table 3.2.2 and the calculated flow for each nozzle at 100% water flow gives the settings in table 3.2.1 for use in the simulation. These numbers are calculated by interpolating the pressure table of the nozzles and using the maximum total flow rate divided by the total number of nozzles according to the BOM.

Table 3.2.1: Flow rate and bar setting used in the simulation for different percent settings in the test

		litre/min	bar
100%	small	0.410	0.161
	big	0.448	0.094
50%	small	0.205	0.081
	big	0.224	0.047
10%	small	0.041	0.016
	big	0.045	0.009

Bellow are all the same tests Benteler did in their P55 quench box in the simulation software QForm. The nozzles used are the GYU 1310 T1 (the smaller of the two) and the GYU 1581 T1. These are 90° spread nozzles with a deviation angle of 5°. This means the angle γ_w, as seen in figure 3.2.3, is 90°, and angle γ_h is 5°. The flow table for these nozzles is then added into QForm along with HTC values that QForm, the company, provided.

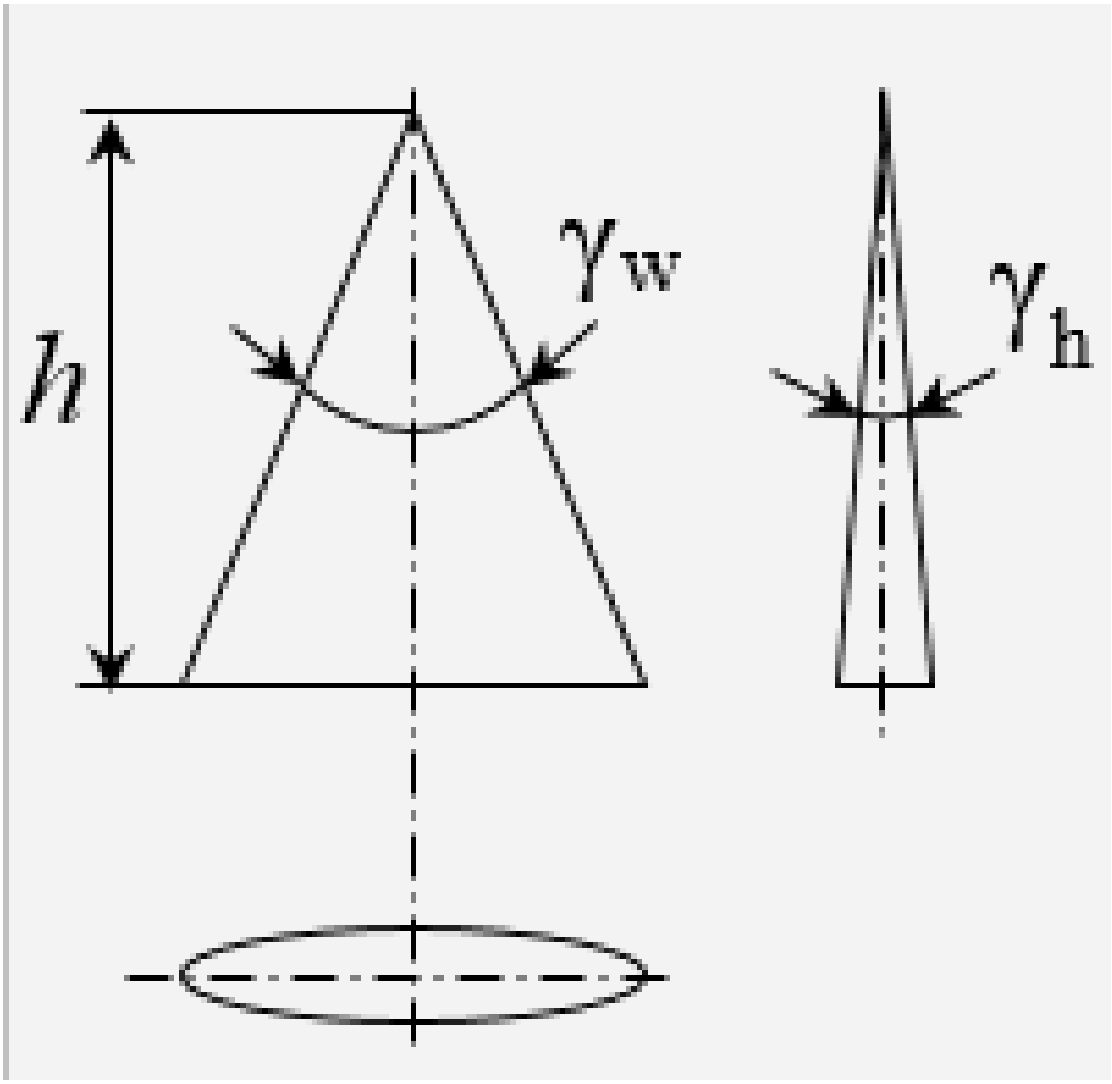

Figure 3.2.3: Figure showing parameters needed in QForm

The values that must be supplied to the QForm software to make a nozzle are the two angles stated above to give the geometric shape of the fluid fan. It also needs the orifice equivalent diameter of 1.7 mm for the smaller and 2.3 mm for the larger nozzles, and the table 3.2.2 of the liquid flow rates for a given liquid pressure. The values used for the heat transfer coefficients are also in the appendix in table .0.1.

There are also air slits/nozzles on all sides, which are not used in these tests and will remain off when testing is done.

Table 3.2.2: Fluid flow rate for a given nozzle and pressure

	GYU 90 1310 T1	GYU 901580 T1
Liquid pressure [bar]	Liquid flow rate [L/min]	Liquid flow rate [L/min]
0	0	0
0.5	1.27	2.37
1	1.79	3.35
1.5	2.19	4.11
2	2.53	4.74
3	3.1	5.81
4	3.58	6.71
5	4	7.5
7	4.74	8.87
10	5.66	10.6

CHAPTER

FOUR

RESULTS

In the result section, the results from each of the different tests and simulations will be reviewed and shown to give an overview of the data gathered during the tests.

As this thesis is mainly focused on the cooling of the profiles and not the extrusion, there will be less data and focus on the numbers gathered here and more to verify that they work and are worth pursuing further.

4.1 Extrusion Experimental Results

Figure 4.1.1 is a graph showing the exit temperature of the test profile. As the extruded profile exited the extrusion press, the temperatures from the top surface of the profile were measured using an infrared camera. As can be seen in the graph, these are not consistent data. When looking at the numbers, they fall to a flat 200.174 °C at the lowest line, indicating that it is a measuring fault or some other data corruption. So if we ignore this most likely corrupt data and the point in between that is most likely also corrupted data, but that is in some transient trying to fix itself. The temperature in the points looks reasonable with

the expected noise. They lie in the 540 range ±5 °C.

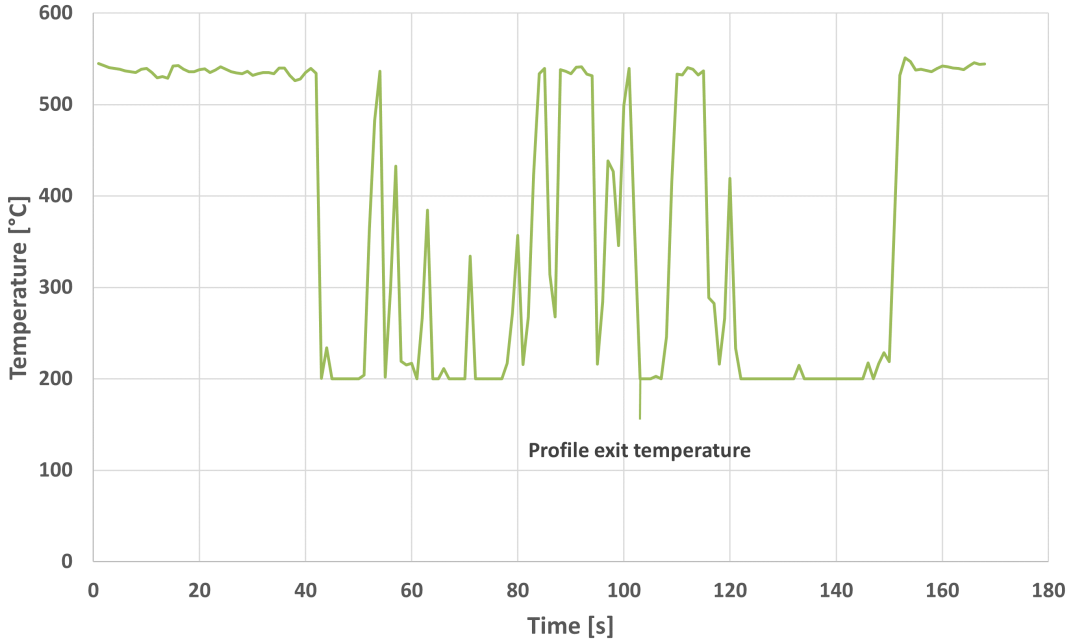

Figure 4.1.1: Temperature measured at extrusion press exit by IR camera

Figure 4.1.2 graphs the forces in tonnes pushing the ram. The shape of the graph is characteristic of what is happening inside the chamber. The first part before the peak is the ram pushing the billet fully into the chamber and squeezing it outwards a bit as the billet is usually smaller than the chamber, so it is easier to insert. This causes a sharp rise when the ram first contacts the billet and a slower rise as the ram squeezes the aluminium outwards to fill the chamber. Then when it reaches the peak, the forces come from it, filling the extrusion die, fighting the friction between the container and billet and all the internal share between different dead metal zones and flowing metal. Lastly is the gradual decline in forces as the billet is pushed out, and there is less area for the billet to contact the container giving less friction to fight. Depending on how much of the butt-end is left or tried pushed through the die, and it can also give a small force bump at the end of the press.

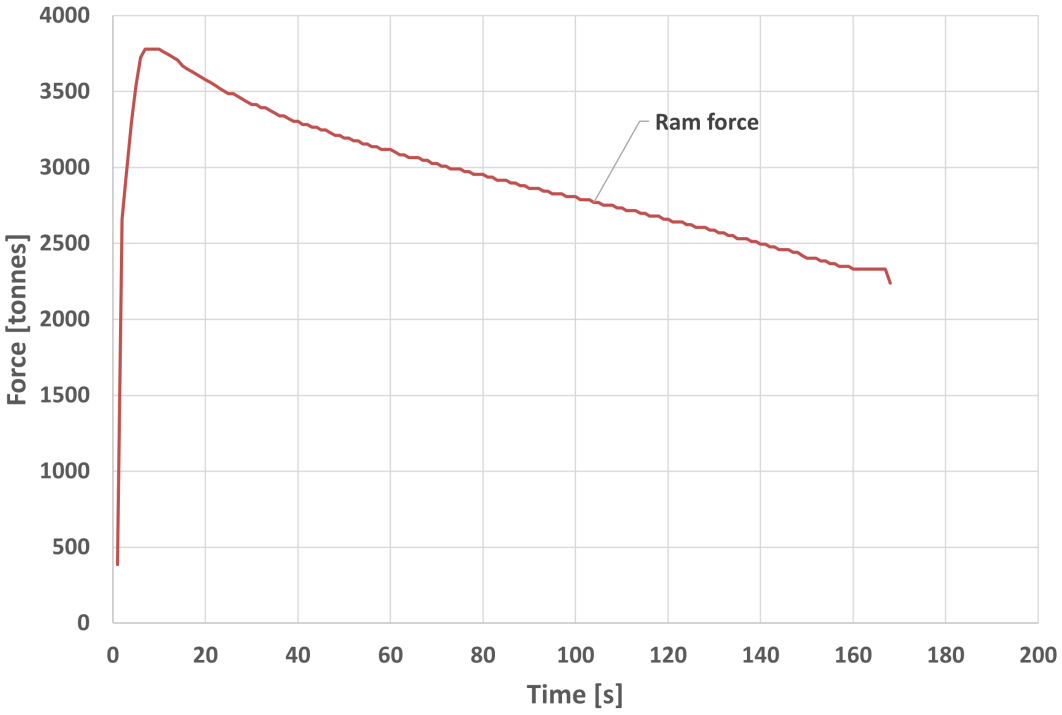

Figure 4.1.2: Ram force during extrusion

4.2 Extrusion Simulation

Figure 4.2.1 shows the profile's average temperature at the bearings exit. These are taken as the average temperature of each simulation step, showing the average temperature over time from the start to the end of the extrusion.

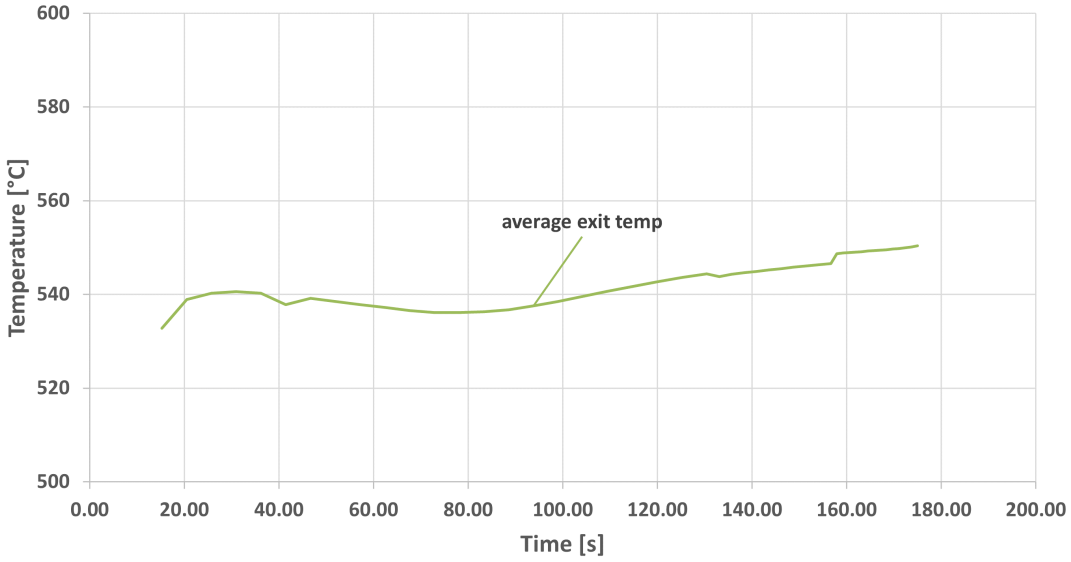

Figure 4.2.1: Graph of average exit temp for each step of extrusion simulation

Figure 4.2.2 shows the ram force in tonnes for the simulation.

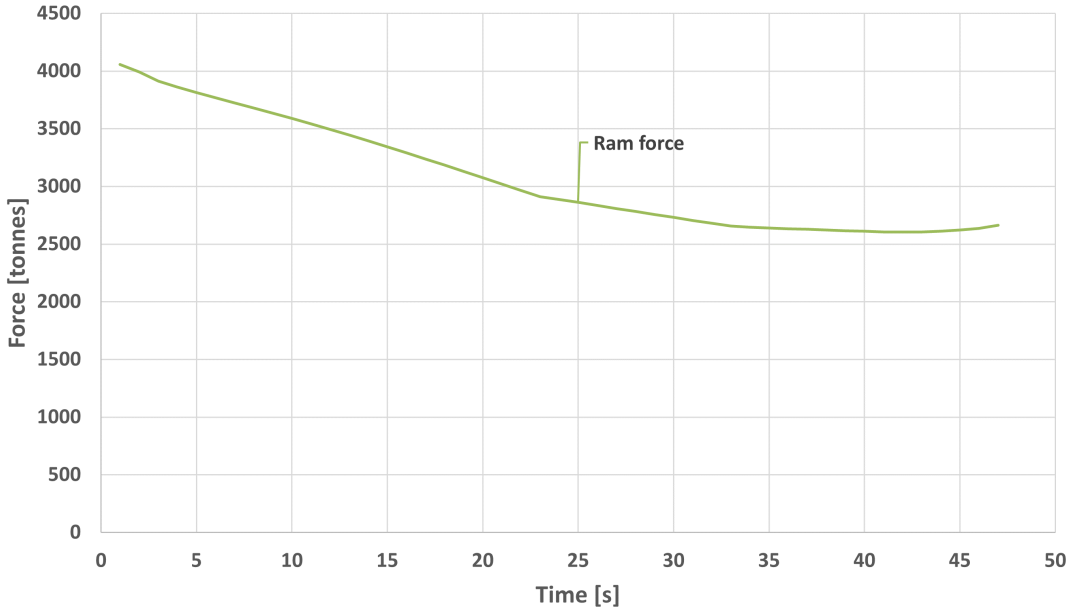

Figure 4.2.2: Graph of ram force from simulation

Figure 4.2.3 shows a cross-section of the temperature gradients when the simulation has reached a steady state condition. This is also the cross-section used in the quench simulation to get a realistic temperature and stress cross-section when running those simulations.

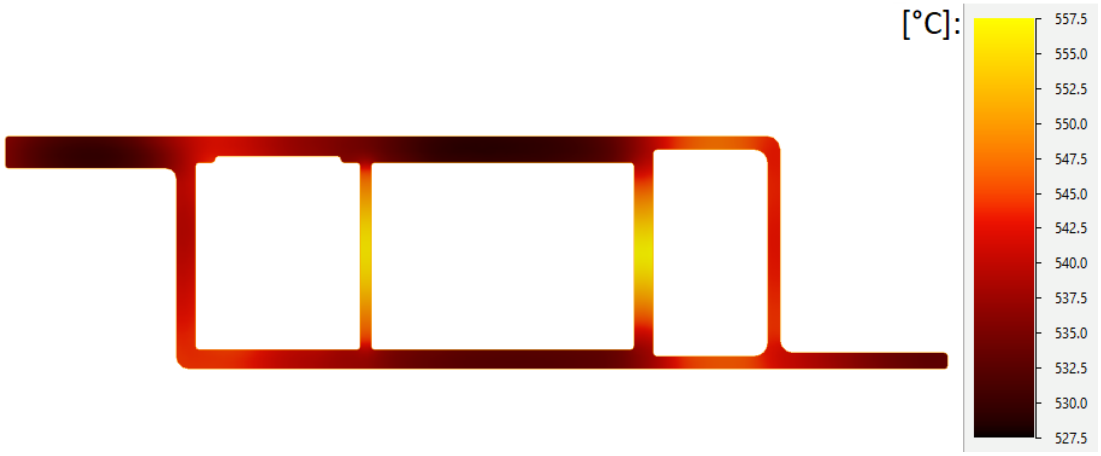

Figure 4.2.3: The temperature gradients in the profile before cooling in [°C]

4.2.1 Material Parameter Comparison

As found in the paper (Medvedev et al. 2020), the material parameters included with QForm are not the most accurate. So, some other material parameters are acquired to test and compare to the included material parameters. Figure 4.2.4 is a graph showing the material parameters that were included with QForm, material parameters found in the study (Pinter and Mehtedi 2012), parameters that Benteler provided and also one simulation running using QForm finer temperature calculations.

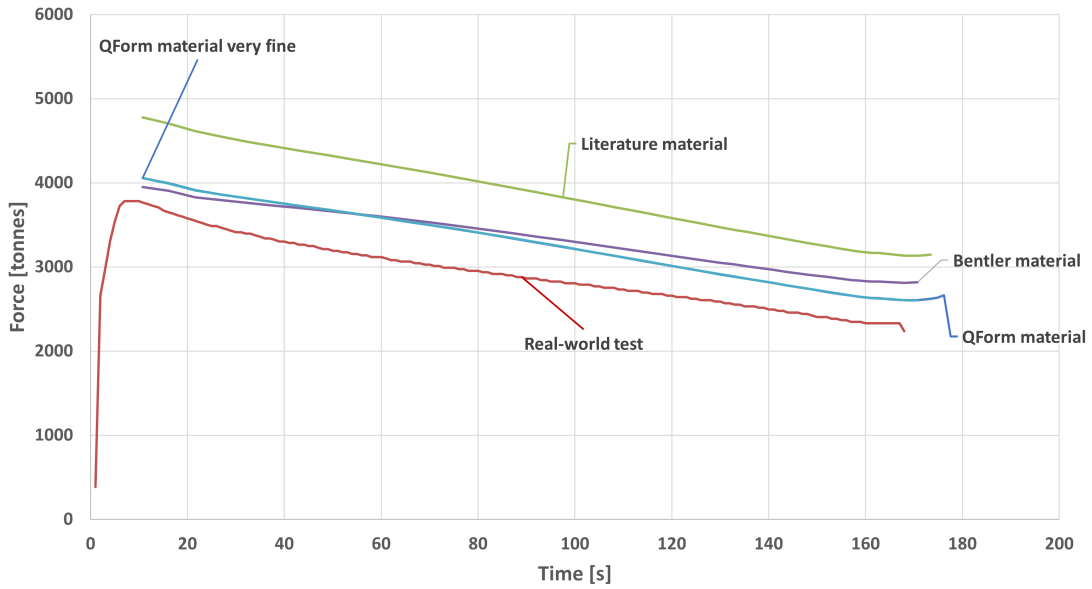

Figure 4.2.4: Different material parameters used for the same simulation setup comparing ram load

The worst material parameters are the parameters obtained from the paper by Pinter and Mehtedi 2012, which are significantly higher than all the others. As for the Benteler-provided material parameters, they are closer to real-world data. However, they are still higher and shallower in comparison, giving a difference of 4.5% at the highest load but a whole 20.6% at the low end, leaving the QForm material as the closest with a difference of 7.4% and 11.8% at the high and low end of the load. As for the very fine calculation run of the QForm material. The difference is lower than 0.1% to the normal calculation run, but with a 50% longer simulation time, making it not worth the extra time for so little extra accuracy.

The temperature is also an exciting measurement to compare and contrast the different material parameters, so here is the temperature for the same node in 4 different simulations, with the only difference being different material parameters. Figure 4.2.5 shows literature material is the furthest off the real-world data in yellow. The real-world data shown here are manipulated because some corrupted or erroneous data have been removed. Primarily, data points fell to 200.174 °C from one measurement to the next.

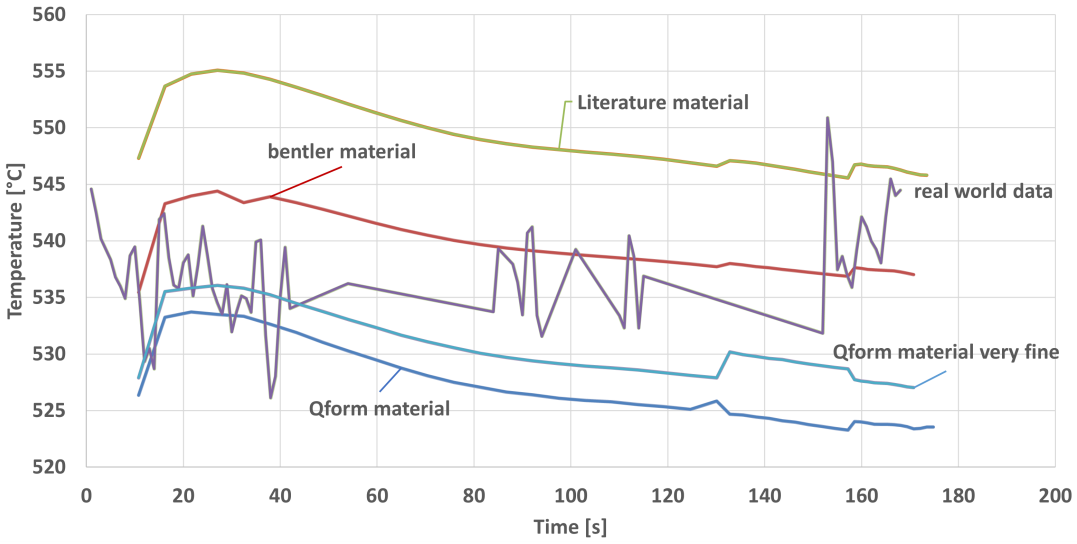

Figure 4.2.5: Different material parameters used for the same simulation setup comparing temperatures at the same node

4.3 Cooling Experimental Results

Table 4.3.1 are the settings used in the different tests. The numbers in the table are the maximum flow rate percentage value for the different nozzles in the cooling station. This maximum flow rate is 86 litre/min for all the smaller nozzles and 94 litre/min for all the larger ones in the cooling station. This gives 0.410 L/min and 0.448 L/min for each small and large nozzle, respectively, according to table 3.2.1 where the calculations for the simulation of the same setup are done. From the table 4.3.1, one can see that most variations of the different options for cooling are tested. Some tests are missing here but have either been done in other places or are similar to others and was skipped by Benteler. Those are P55-1 which is assumed to be the standing wave test, as this one was done with the same profile in a different cooling station, and as it is just running the profile into and out of standing water, the results should be the same. The other test is P55-7, from the results on tests P55-3 and four will give about the same results as test P55-6.

Table 4.3.1: Cooling experiments

test number	Q1 Small	Q1 Big	Q2 Small	Q2 Big
P55-2	10	0	10	0
P55-3	50	0	50	0
P55-4	100	0	100	0
P55-5	0	10	0	10
P55-6	0	50	0	50
P55-8	10	10	0	0
P55-9	50	50	0	0
P55-10	100	100	0	0
P50-11	100	100	100	100
P55-12	0	0	10	10
P55-13	0	0	50	50
P55-14	0	0	100	100
P55-15	10	10	50	50
P55-16	50	50	10	10

4.3.1 Test Result Graphs

The figures below show the temperature of the top side of the test profile as it travels through the quench box. The temperature is as soon as the measuring device (see section 3.1) is placed on the profile and usually lasts 30 seconds which is more than enough for the measuring device to pass the quench box.

Figure 4.3.1 shows the tests named P55-8 to P55-11, where in tests 8 to 10, box two is turned off, and in box one, the water flux is increasing. It also shows tests P55-11, a baseline for the station operating at 100% on all nozzles.

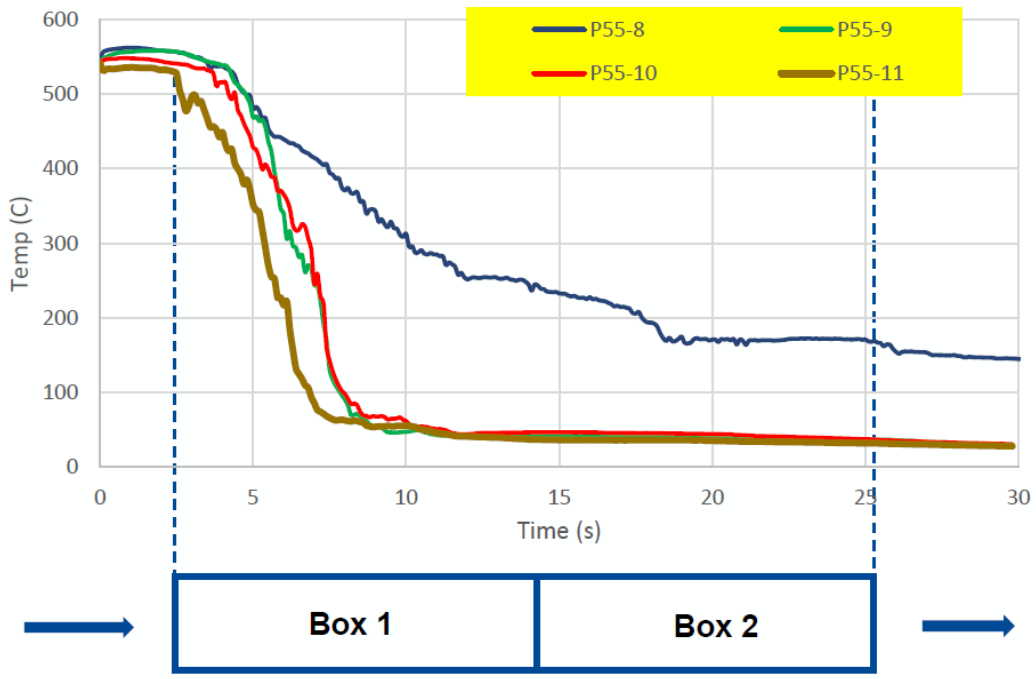

Figure 4.3.1: Test of 0% in box two and increasing flow in box one

Figure 4.3.2 shows tests 11 to 14, which is the first cooling box turned off and the second having increasing water flux. Here too, showing test P55-11 for comparison to maximum cooling.

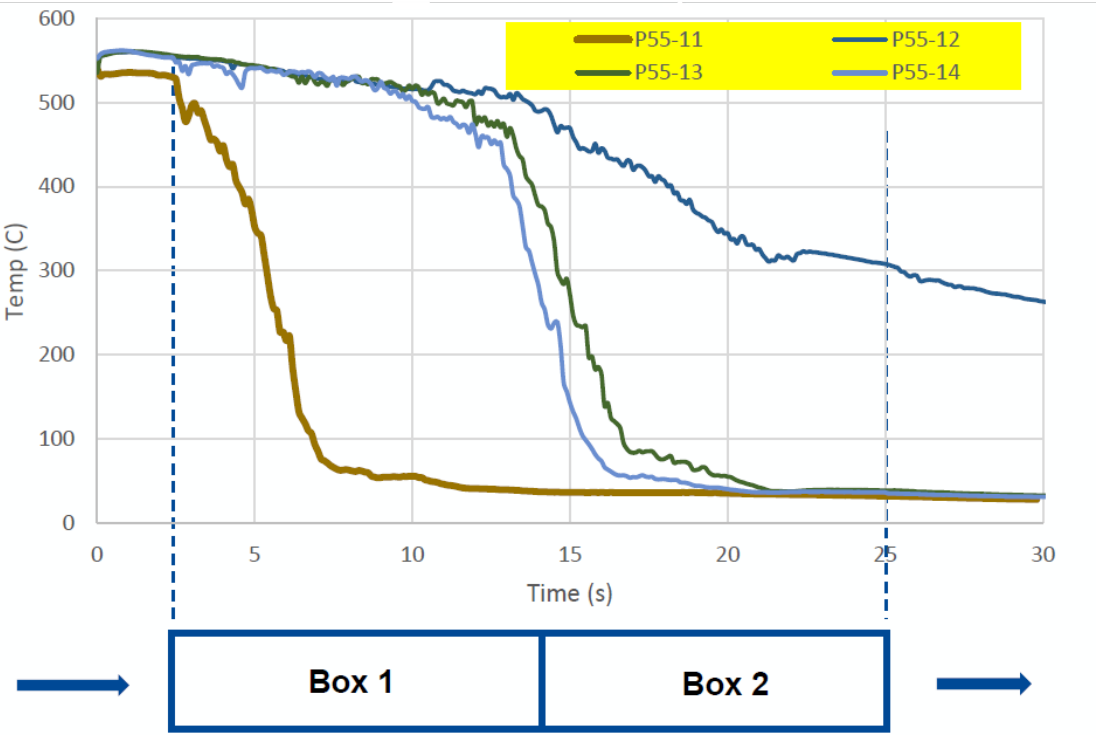

Figure 4.3.2: Test of 0% in box one and increasing flow in box two

Figure 4.3.3 shows the tests only using the smaller nozzles. These are run at 10, 50 and 100% of their maximum output. There are some notable features of the 50% run, where at the start it has the same cooling as the 100% run, before being slower between 400 °C and 200 °C, where it becomes a lot faster than the 100% run and quickly falls 100 °C. Run 11 is also added to the graph for comparison to everything at 100%.

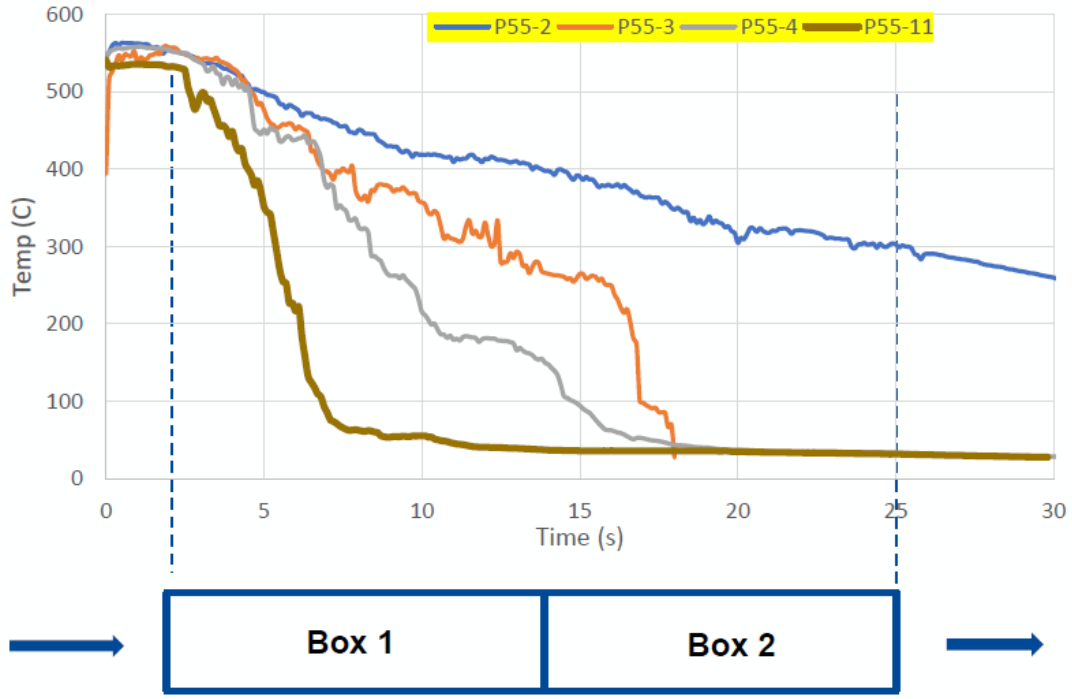

Figure 4.3.3: Testing small nozzles at 10, 50 and 100%

Figure 4.3.4 compares the effectiveness of the large and small nozzles at 10 and 50% water flux. In run 5, the measuring device fell off the profile about 15 seconds into the tests, giving only about half of the quench box worth of data, but the trends seem pretty clear from the data gathered. Run 11 is also added as a reference.

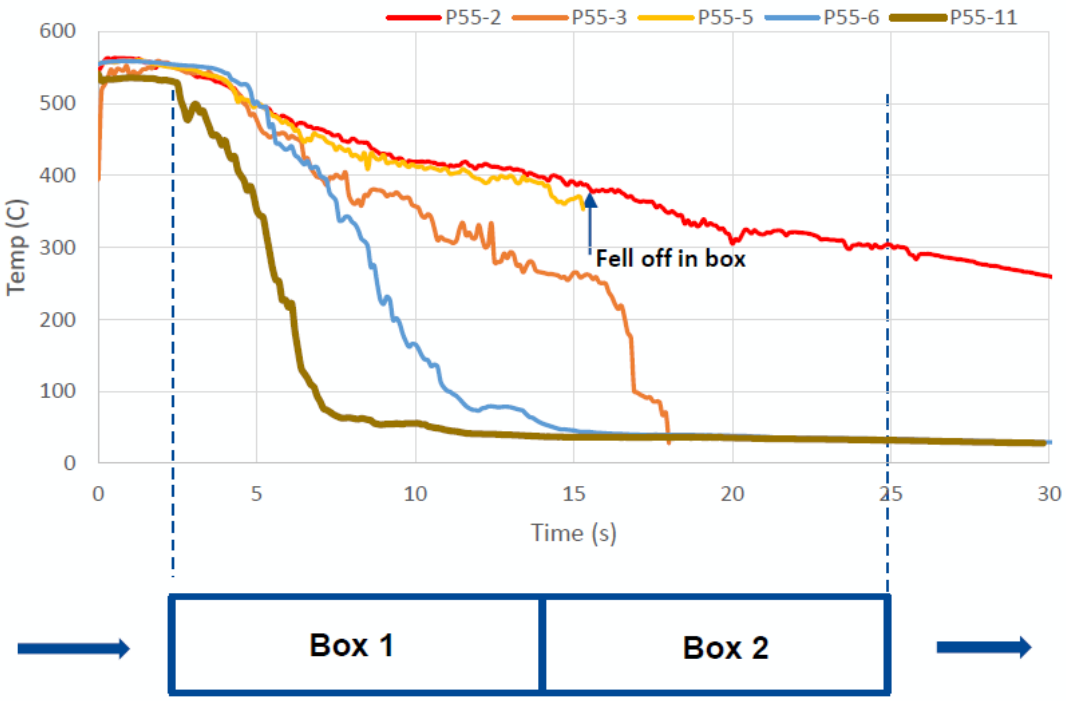

Figure 4.3.4: Comparing small and big nozzles at 10 and 50%

Figure 4.3.5 shows boxes one and two running at 50% separately to show if there is a difference between them. There are tests 15 and 16, where one box is at 10%, and the other is at 50%, to test if there is any benefit to starting the cooling slowly and speeding up later or vice versa.

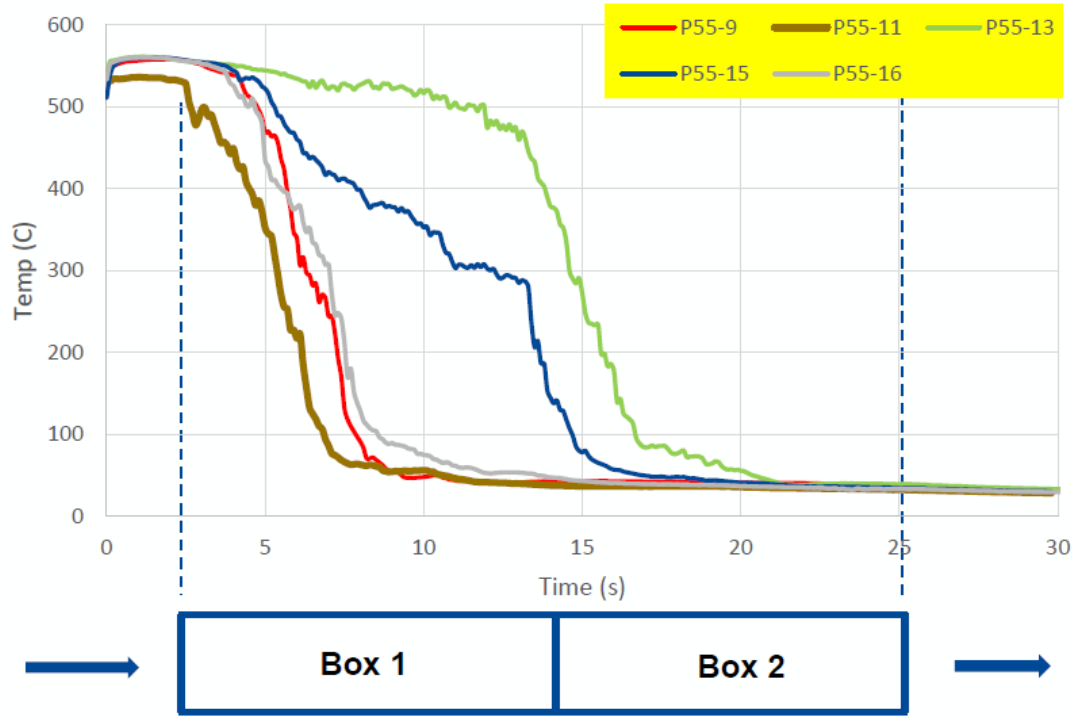

Figure 4.3.5: Comparing box one and two and a combination

Table 4.3.2 repeat the settings used for the different tests and also shows the time it takes for each test to go from 450 to 200 °C in seconds, plus the calculated number of °C per second that represents in cooling capacity. These numbers give a good indication of how good each of the set-ups is at cooling the profile down below its critical temperature. Using the average temperature cooling rate between 450 and 200 °C will more than cover the critical temperature for most alloys, according to a study done by Mackenzie 2020, which is between 400 and 300 °C.

Table 4.3.2: Tests were done with their settings and the time between 450 and 200 °C and the °C per second for that range

	Q1 small	Q1 big	Q2 small	Q2 big	time 450C-200C (s)	cooling rate 450C-200C (C/s)
P55-2	10	0	10	0	39.7	6
P55-3	50	0	50	0	10.3	24
P55-4	100	0	100	0	5.4	46
P55-5	0	10	0	10	>30	<8
P55-6	0	50	0	50	3.8	66
P55-8	10	10	0	0	12.2	20
P55-9	50	50	0	0	1.9	132
P55-10	100	100	0	0	2.5	100
P55-11	100	100	100	100	2.3	104
P55-12	0	0	10	10	27.2	9
P55-13	0	0	50	50	2.3	109
P55-14	0	0	100	100	1.9	132
P55-15	10	10	50	50	7.6	33
P55-16	50	50	10	10	2.5	100
P55-17	10 % air		10 % air		>60	<4
P55-18	100 % air		100 % air		>45	<6

4.4 Cooling Simulation

These simulations are only run through the temperature simulation part of QForms quench simulation. It only calculated the water flux that hits the profile as it moves through the quench box, calculating the amount of heat removed from each node. Because of this, and the profile's direction was not known when being extruded through the quench box, the average temperature of all the outer surface nodes will be used in the result graphs for the simulations.

4.4.1 Simulation Result Graphs

Figure 4.4.1 shows the simulation results from the first quench box having the nozzles set to 10% in simulation P55-8, 50% in simulation P55-9 and 100% in simulation P55-10, there is also simulation result of run P55-11, which is every nozzle at 100%, to give something to compare too.

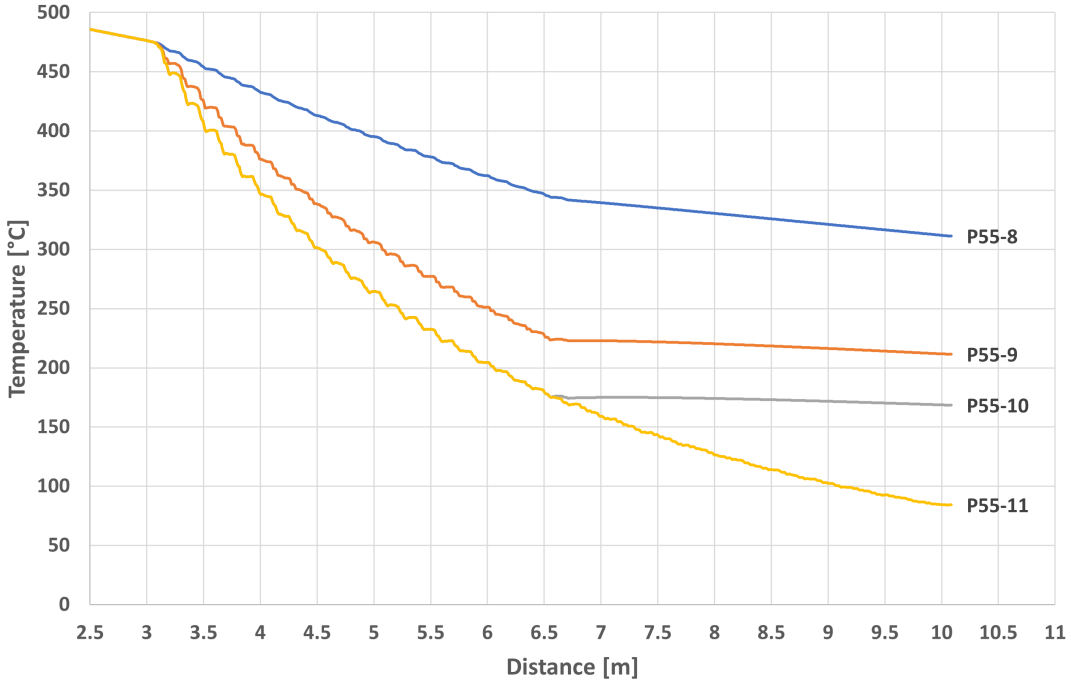

Figure 4.4.1: Simulating nozzles in box one at 10, 50 and 100%

Figure 4.4.2 shows pretty much the same as 4.4.1, but this time it is box two instead of box 1, giving a longer air cooling time before the water starts cooling.

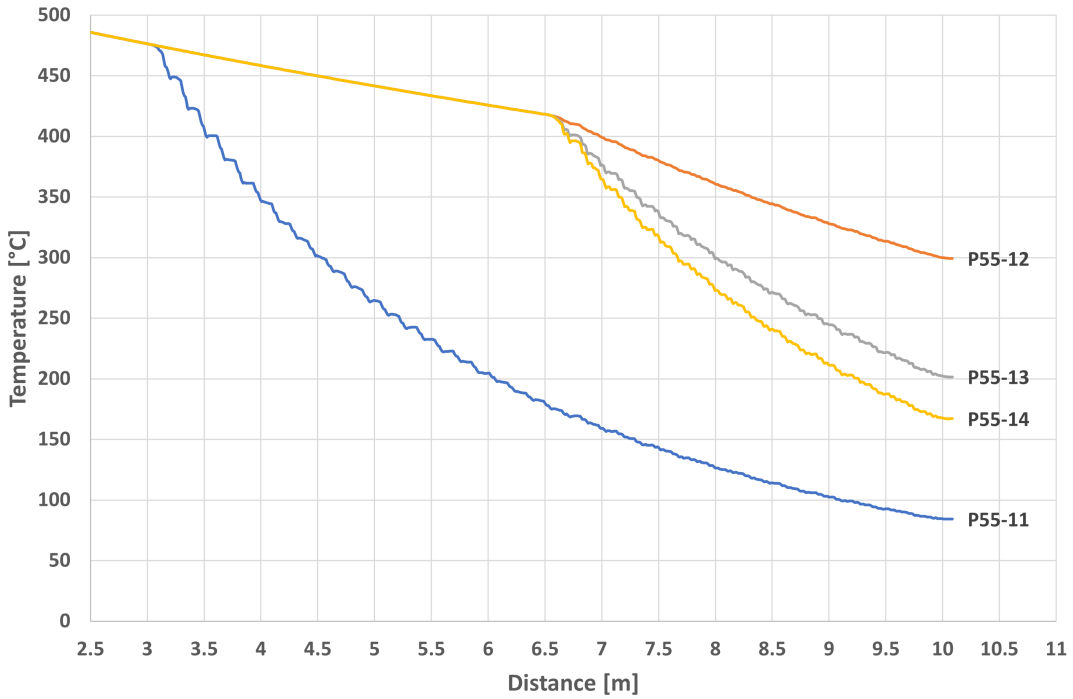

Figure 4.4.2: Simulation result of box two running at 10, 50 and 100%

Figure 4.4.3 shows all of the small nozzles running at 10% in run P55-2, 50% in run P55-3 and 100% in run P55-4. Run P55-11 is also added in for reference to everything at 100%.

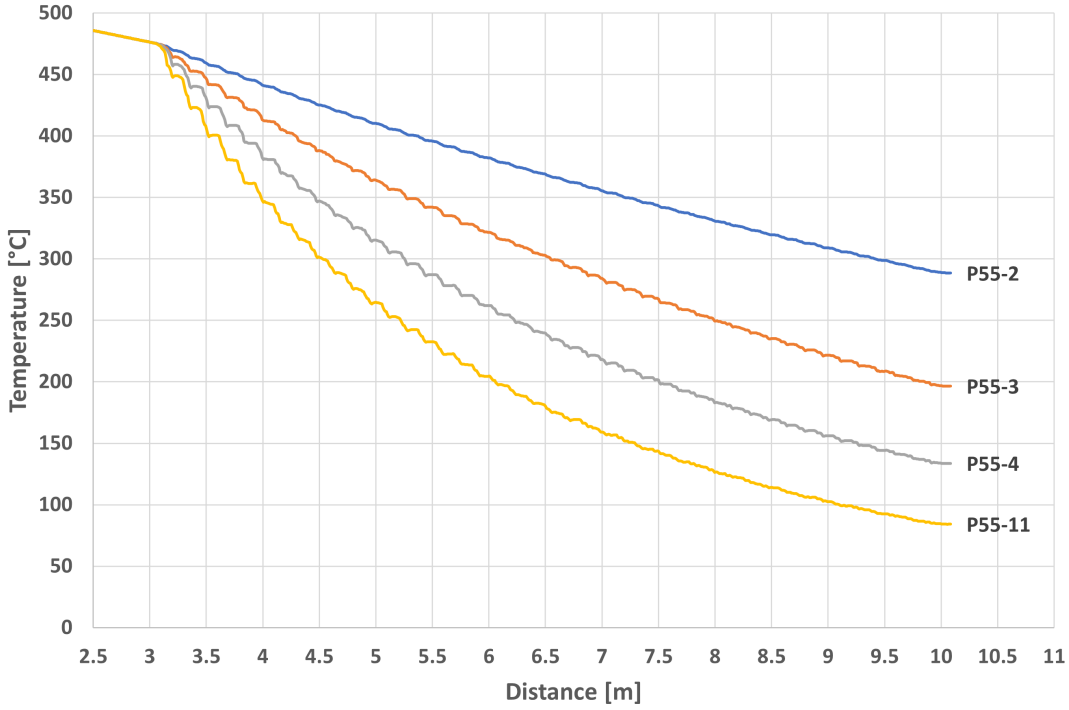

Figure 4.4.3: Simulation of small nozzles at 10, 50 and 100%

Figure 4.4.4 shows all of the large (P55-5 and P55-6) and small (P55-2 and P55-3) nozzles running at 10 and 50%, giving a comparison between cooling effectiveness of each type.

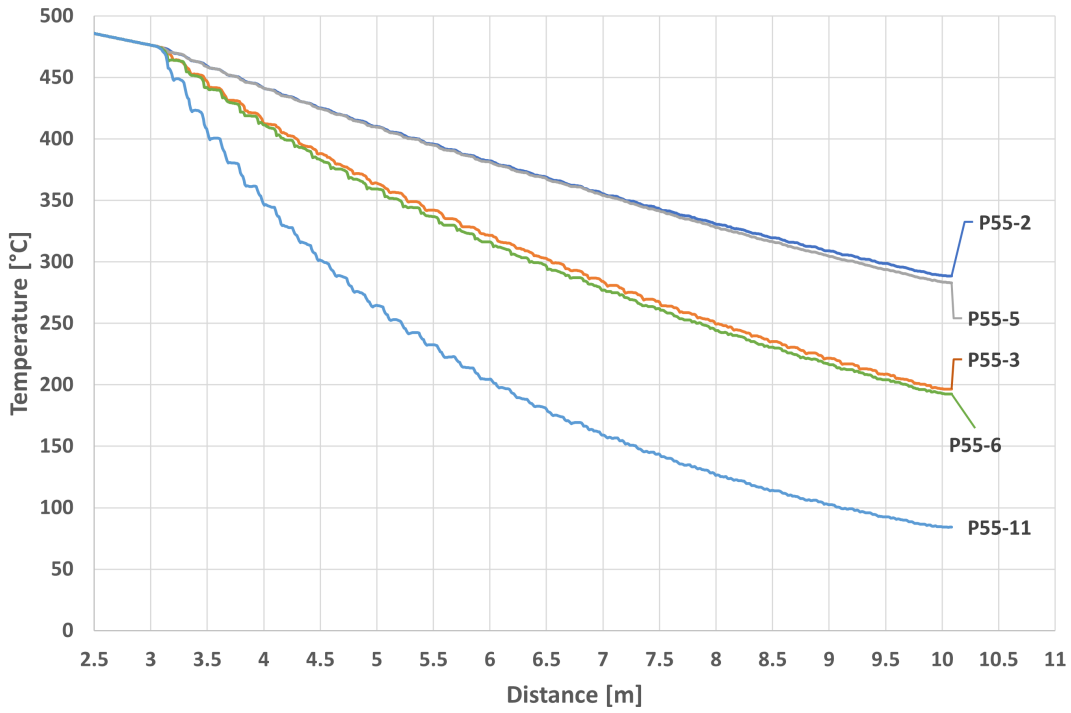

Figure 4.4.4: Comparason between large and small nozzles at 10 and 50%

Figure 4.4.5 shows box one (P55-9) and two (P55-13) running at 50% each, and in simulation P55-15, box one is set to 10%, and box two is set to 50%, which is then flipped in run P55-16.

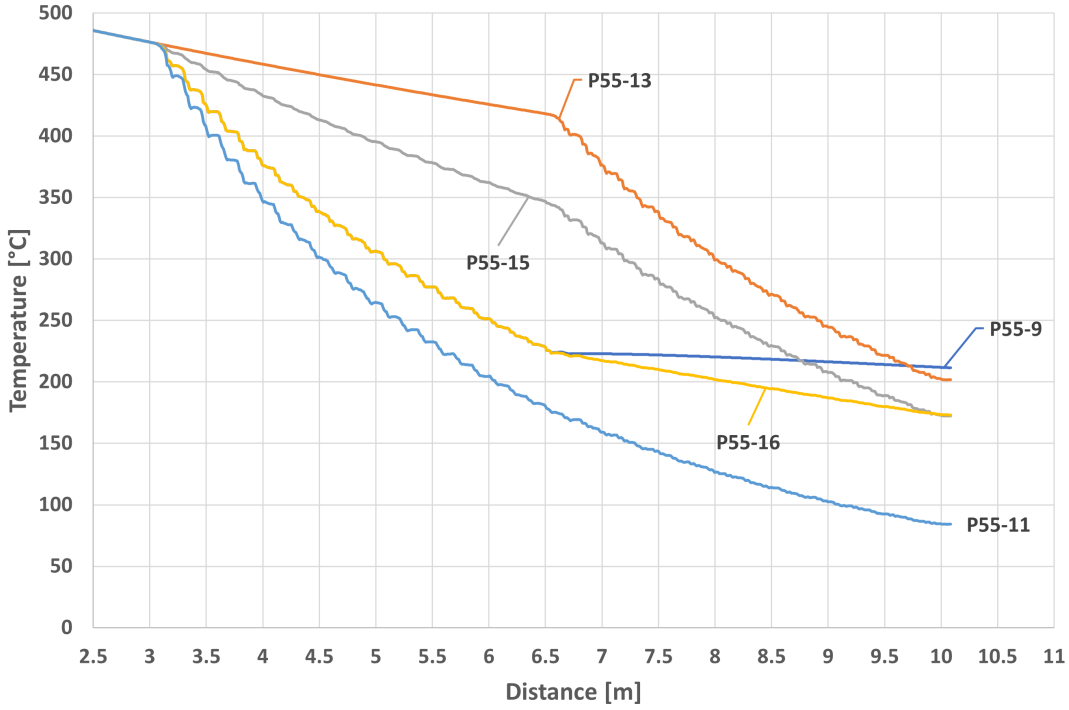

Figure 4.4.5: Comparison between box one and two, plus a combination of both

Table 4.4.1: Table of the different simulation runs with the cooling times from 450 °C to 200 °C and the cooling rate in °C/s

	Q1 small	Q1 big	Q2 small	Q2 big	time from 450C-200C (s)	cooling rate 450C-200C (C/s)
P55-2	10	0	10	0	>19.4	>12.9
P55-3	50	0	50	0	19.7	12.7
P55-4	100	0	100	0	12.9	19.4
P55-5	0	10	0	10	>19.4	>12.9
P55-6	0	50	0	50	19.3	13
P55-8	10	10	0	0	>19.9	>12.6
P55-9	50	50	0	0	>20.9	>12
P55-10	100	100	0	0	8.8	28.4
P55-11	100	100	100	100	8.8	28.4
P55-12	0	0	10	10	>17.3	>14.5
P55-13	0	0	50	50	>17.3	>14.5
P55-14	0	0	100	100	14.7	17
P55-15	10	10	50	50	17.2	14.5
P55-16	50	50	10	10	14.9	16.8

Table 4.4.1 shows the time between the average surface temperature of the profile hitting 450 °C and reaching 200 °C. This gives an excellent single comparison number between the tests that have been done and the simulations that have been run. For the runs that do not hit 200 °C before the profile is out of the quench box, there is added > symbol to clearly show that it did not reach 200 °C inside the quench box.

4.4.2 Heat Transfer Graph

Figure 4.4.6 shows the HTC values given by QForm and used in this thesis. The plot shows the "standard" setup shown by QForm training videos where the different graphs represent different surface temperatures for the aluminium. And for how this is flipped in figure 5.2.6, the graphs represent different liquid flux densities, and the x-axis represents different surface temperatures. This does seem like the more likely case, but they have been used like was shown in the training material.

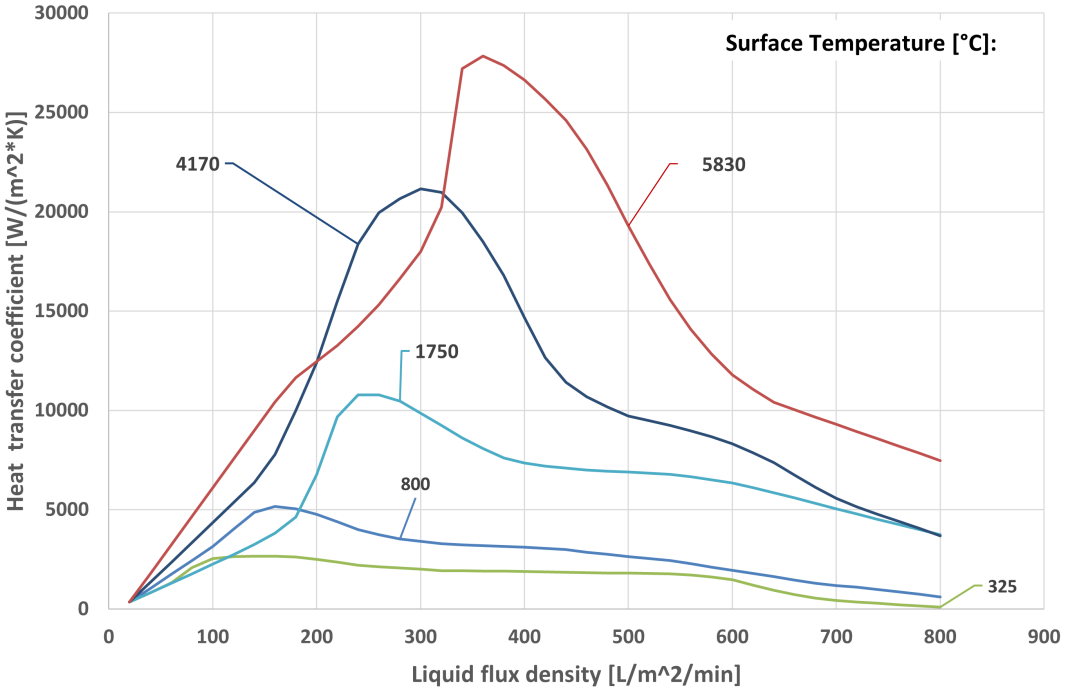

Figure 4.4.6: A plot of the HTC values used, with the standard axis

CHAPTER

FIVE

DISCUSSION

Comparing and contrasting the results obtained earlier and attempting to make sense of them.

5.1 Comparason Extrusion Data

For the force comparison between the real-world data and the simulation data, there is a clear few percent difference in the results for the whole simulation run. Still, they are consistently above the real-world data. And with what was discussed and figured out in the material parameter simulations and studied in the study by Medvedev et al. 2020, the material parameters that are supplied with QForm are not always the most accurate compared to getting material data for the actual material being used and using those for the simulations. Benteler did provide some material parameters that were compared with material parameters from both literature and QForm in 4.2.1 where the QForm material parameters were consistently closest to the real-world data.

In the study by Medvedev et al. 2020, they found that the material parameters in QForm give higher stress and more forces compared to the material parameters

they found based on experimental data and curve-fitting that data to the Hansel-Spittel material model. When running with their material parameters, their results agreed with the experiments ($R^2 > 0.99$). The reasons our results differ compared with the real-world data can be from these material parameters being different. These differences can come from slight chemical differences in the alloys, variations in manufacturing processes and testing equipment and techniques. It can also be because of there being differences in the dies both from the natural wear of the die during use but can also come from changes that have been done to the die and especially bearings to get a better and straighter to extrude based on tests and the experience of the operators.

As seen in figure 4.1.1, there is quite a bit of garbage data among the temperature data gathered from the IR camera during the real-world test that Benteler did. The temperature data that can be extracted from the extrusion simulation does not start much into the extrusion at about 15 seconds, as they are when the chamber and die are being filled. These simulations are somewhat possible to do with a different simulation mode, called profile flow simulation, which focuses a lot more on the actual flow of material and the startup and optimization of a die, while the full billet simulation that has been used in this thesis is more for getting temperature data for the entire length of the billet and seeing how the billet as a whole act in terms of forces and temperatures.

With that in mind, figure 5.1.1 compares the average temperature of a cross-section from each step in the simulation and the data points that Benteler provided from the IR camera they had pointed at one of the wide sides of the profile. Both real-world data are noisier to work with, and IR cameras have a $\pm 2\%$ accuracy at room temperature, which will be pretty substantial at higher temperatures—giving good reason to believe that the simulation is reasonably accurate.

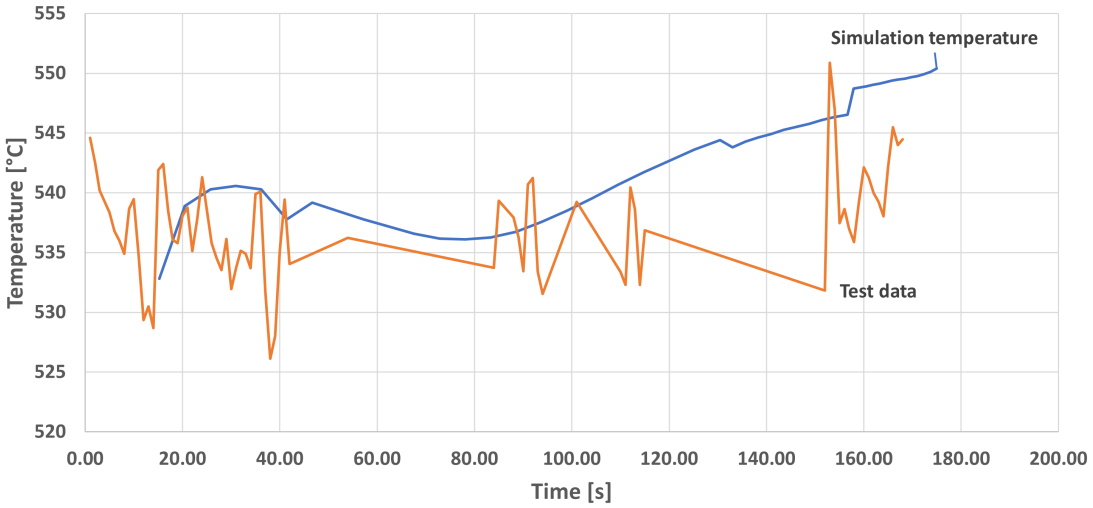

Figure 5.1.1: Temperature comparison between test and simulation results

Figure 5.1.2 shows the force in the ram in both the real-world test data provided by Benteler and the simulation data obtained from using the die files and extrusion parameters provided by Benteler. It is the same with these data as with the temperature data shown in figure 5.1.1 that the simulation data does not show the initiation phase of the extrusion, at least not in this mode. Instead, it starts at the pressure peak of the extrusion and more or less follows the real-world data pretty well, with the asterisk of it being offset by about 9% for the whole extrude. Which with better material parameters can be improved, but that will need some trial and error with different material models and parameters.

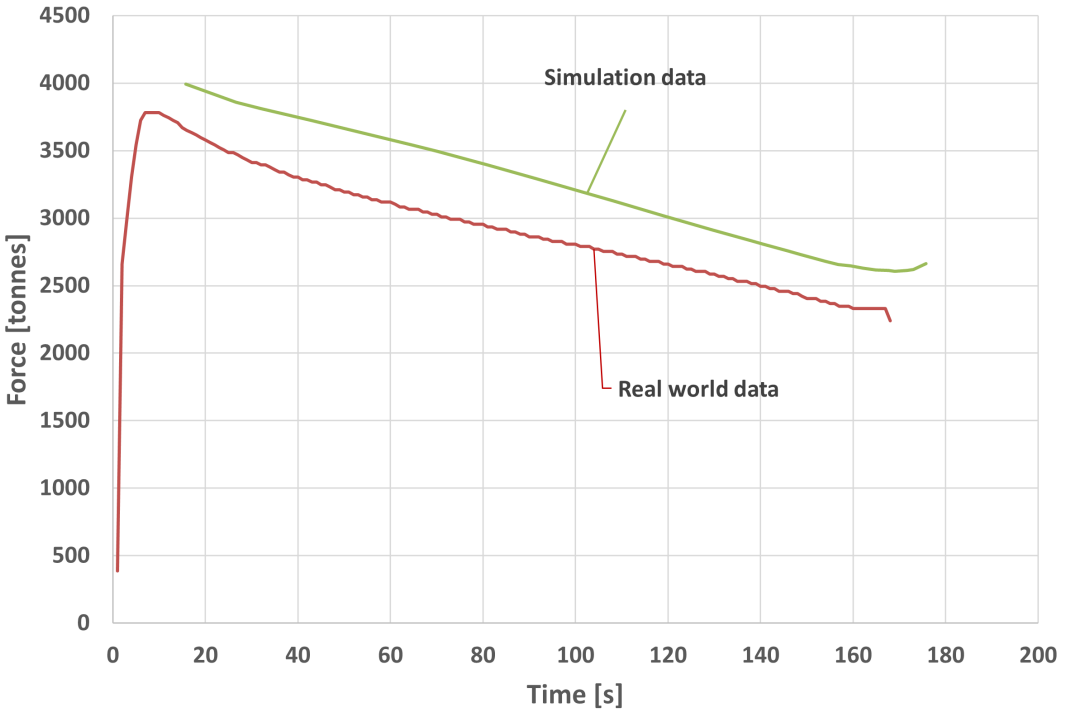

Figure 5.1.2: Force comparison between test and simulation results

One of these parameters Benter was not entirely confident about that being the temperature of the dummy block sitting between the ram and the billet itself. This has not been a big problem in the real world as the block has just heated up from the heat generated in the billet and the forces acting. Still, in the simulation, the temperature of "outside elements" means anything that is not the billet, die or die backing. It stays constant the whole simulation and removes heat at a rate proportional to the temperature difference between it and the billet or dies. This means that with a starting temperature of 260 °C, as provided by Benteler, the whole billet pretty much got cooled down to not much higher than that temperature giving way to high forces. This was fixed before any of the test data seen here was taken. Still, it is an excellent example of things that may not do much in the real world that can have enormous consequences in simulation, depending on how that simulation was coded and made. The final solution for this specific problem was setting the temperature of the dummy block to the same temperature as the temper on the billet at 400 °C, which was also the same temperature provided for a different profile and setup by Benteler where they were

sure about the temperature of it.

5.2 Comparing Cooling Data

As the real-world cooling test data is provided, the entire data from leaving the die bearings to the end of the cooling box was not provided. Instead, the cooling data between 450 and 60 °C is shown in the comparison charts in the discussion section. The entire temperature profile can be seen in the graphs provided and shown in the result section for real-world cooling data.

This quirk of the data will also give some inconsistencies in the starting place of where the real-world test data starts dropping. This comes from the profiles on average not reaching 450 °C before they are into the quench box, so that is where they are moved too. Still, for some tests, the water quenching does not start before box two or reaches 450 °C in the middle of box one, making it impossible to shift these tests to the right place for these test without further cluttering the data as this sifting will be done based on loosely educated guesses. So all the real-world data is shifted so they start at 450 °C at the start of quench box one, and for those tests where this data that was provided point is most likely wrong, this will be commented in the text.

The first thing to notice in figure 5.2.1 is the significant difference between the real-world test, which are pretty much straight lines from 450 °C to 100 °C for both 50 and 100%. The simulation temperatures go down along a much shallower hyperbola-shaped graph, where the per cent setting on the nozzles determines how shallow that graph is.

One notable point is how close the number 8 real-world test corresponds to the number 9 and 10 simulation results. The number 8 test is the 10% setting of both nozzles in the first box, and it is 50 and 100% for 9 and 10, respectively. This may be a strong indication that the amount of water that is getting sprayed in the test is too low compared to what was used in the real-world test, which from the limited data to go by, maybe a good possibility.

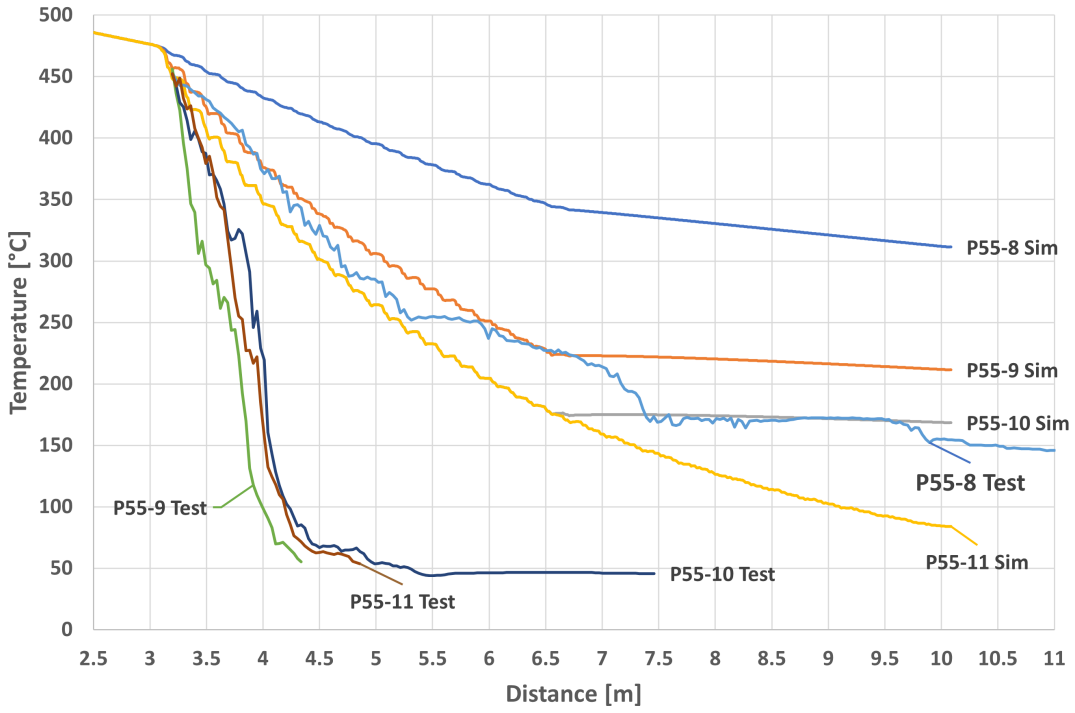

Figure 5.2.1: Comparison between simulation and test data in test 8 to 11

In the graphs in figure 5.2.2, the starting point of tests 12 to 14 is highly likely wrong as they are not getting any cooling before the start of box two, but the steepness of the graphs between the simulated data and the real-world data is equally stark here and in tests eight too eleven. The results for test twelve and simulation thirteen do look like they have similar slopes, similar to how test eight and simulation nine look similar.

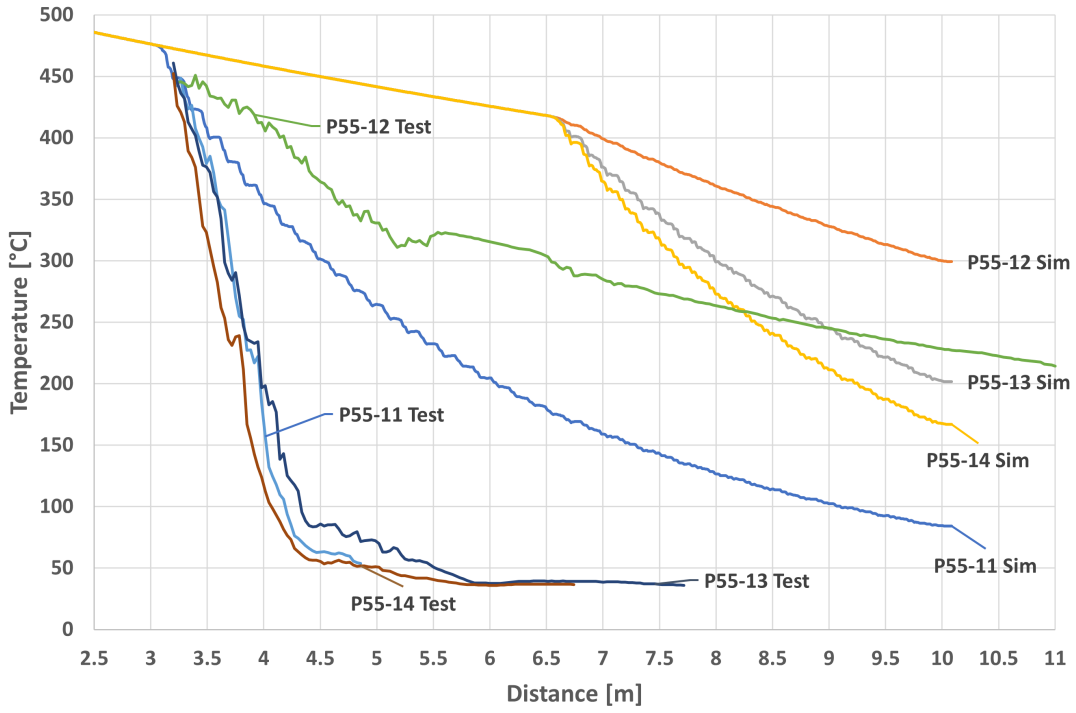

Figure 5.2.2: Comparison between simulation and test data in test 11 to 14

Next are graphs comparing the first three tests, tests two to four, in figure 5.2.3. Where test and simulation two are pretty much equal, which is interesting to note when compared to test three, which is a lot closer to simulation four until about 250 °C and the temperature rapidly drops to 100 °C. Test 4 is quite a bit steeper than even simulation eleven. Still, the more notable point is that it plateaus at the same temperature where test three drops the fastest in temperature. However, this is most likely because of the transition between boxes one and two, and the graphs are not synchronised.

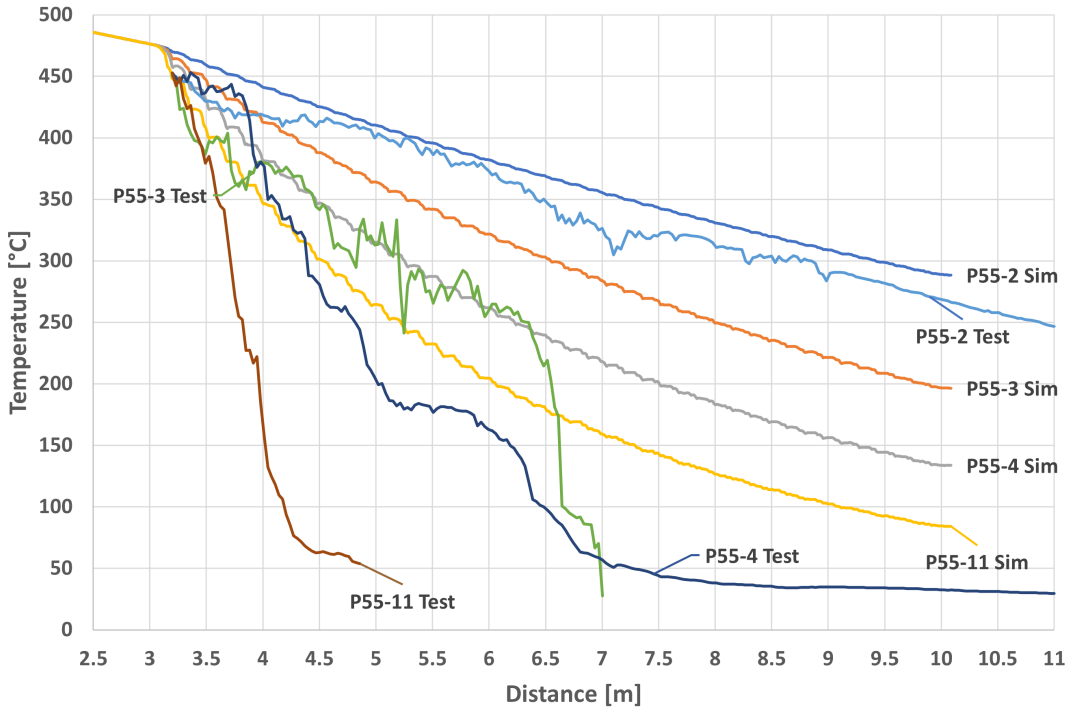

Figure 5.2.3: Comparison between simulation and test data in test 2 to 4 plus 11

In figure 5.2.4 are graphs comparing the large and small nozzles being set to 10 and 50%. Firstly, the temperature measuring device fell off the profile in test 5, which is why it suddenly stopped. But from the data gathered, it can be seen that tests 2 and 5 are pretty similar in cooling performance and are also not far off the simulation results for simulations 2 and 5. When it comes to test 3, it is also quite similar to simulation runs 3 and 6 if it was shifted a bit to the right, though that is only until it gets to about 250 °C, where the temperature drops off a cliff. Lastly, test 6 is closer to test 11 than any of the simulations.

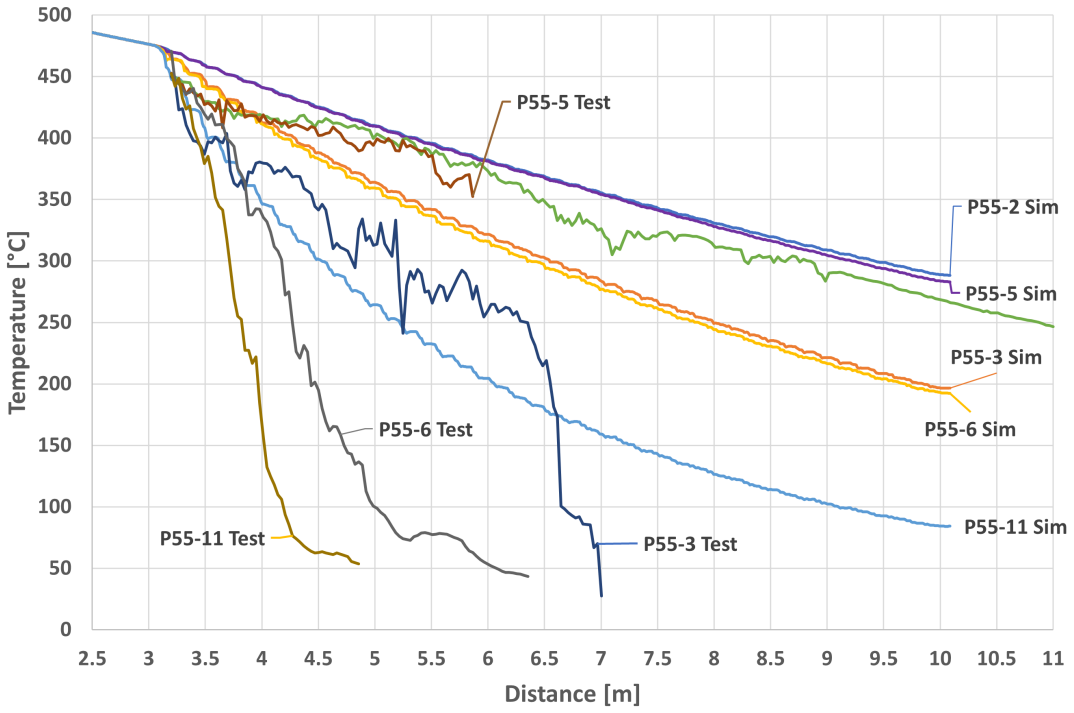

Figure 5.2.4: Comparison between simulation and test data in test 2, 3, 5, 6 and 11

Figure 5.2.5 shows another example of the simulation set to 50% is pretty similar to a real-world test running at ten% with test 15 and simulations 9 and 16 before the temperature rapidly drops when test 15 gets into quench box two. As for the rest of the tests, they are pretty much cooling at similar rates, be they at 50 or 100%.

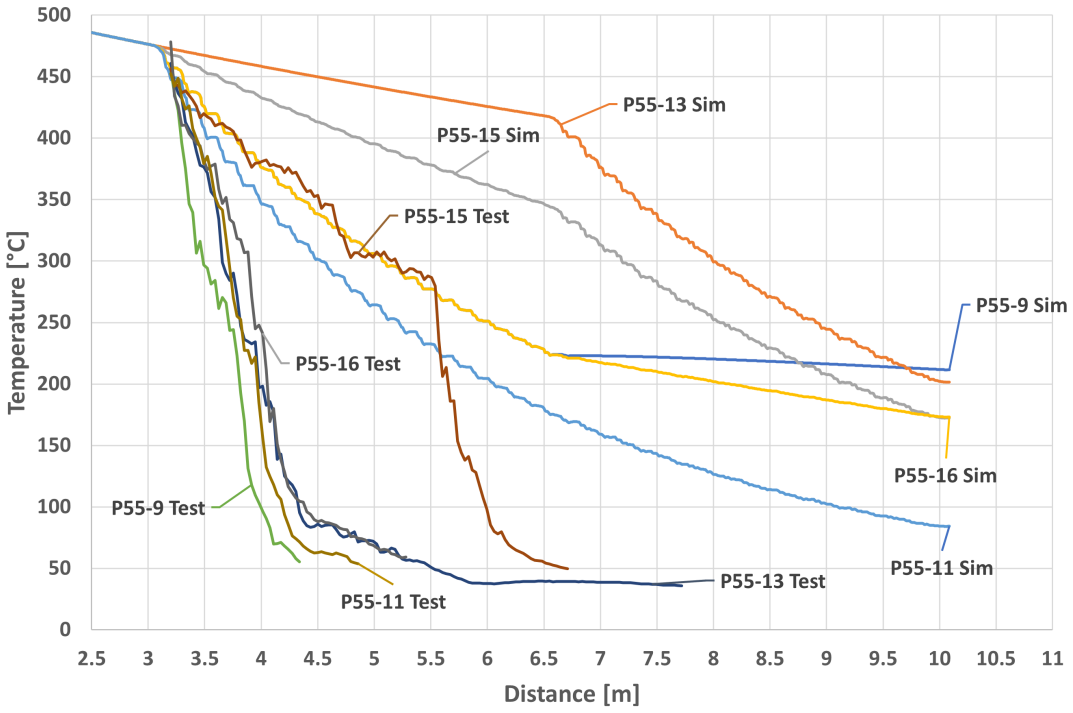

Figure 5.2.5: Comparison between simulation and test data in test 9, 13, 15, 16 and 11

Another possibility is the HTC data from QForm being either inputted with the wrong units or the values being wrong. A comparison between the HTC values being what was shown in the training material provided by QForm shown as the standard and the flipped is shown in figure 5.2.6, where it can be seen that the flipped values do give some faster cooling of the profile with the nozzles running at the calculated 100% setting. There is also a comparison between running the standard HTC values with ten times higher pressure and both higher pressure and flipped HTC values. The last graph showing ten times pressure and the HTC values flipped is starting to look much more like the test result for test 11 with the nozzles running at 100%.

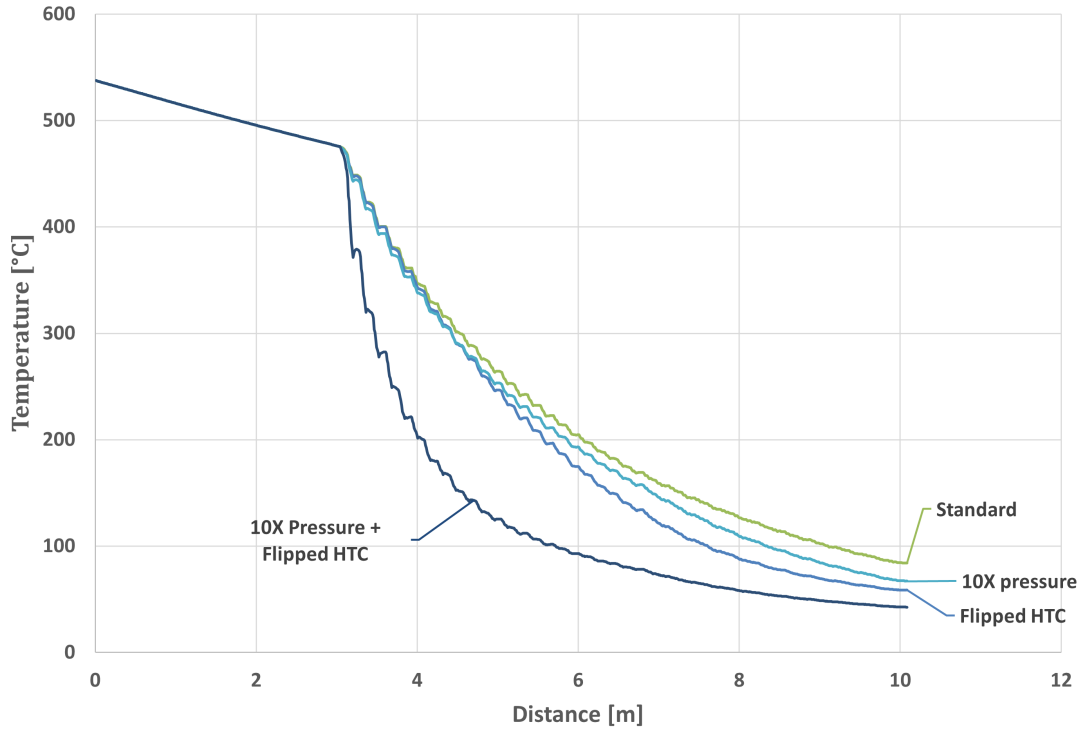

Figure 5.2.6: Comparison between standard and flipped HTC values, plus higher pressure/waterflow

5.3 Future work

Work that must be done to improve the results for the extrusion setup is, at a minimum, getting more specific material parameters for the material being simulated on and used in the extrusion. The same goes for temperature parameters being used together with the HTC values that each specific press can do. Though the default values are not too far off, they are done conservatively so that the simulation is a worst-case scenario.

For the quenching simulation, there is more work to be done. The first is getting the correct setup of the HTC values so they are not flipped (if that is the case). The second is doing a test on a quench setup and getting the correct flow or pressure for each nozzle, so these values are much closer to the source and not values that are calculated back and forth many times to get the relevant value.

Some tests or experiments need to be done to compare the distortions and twisting of profiles between the simulations and the real-world quenchings as that is data not available from the real-world test that was done.

CHAPTER

SIX

CONCLUSIONS

With suitable material parameters for the correct material for what is being extruded, QForm will give reasonably accurate simulations of the extrusion process. This also required that the other parameters are filled in correctly and that temperature parameters do not change during the extrusion.

For industry, this means they can skip or at least significantly reduce the trial and error process of getting the die to have the proper geometry and bearings to have the correct length for different profile parts to give a consistent and straight extruded beam.

This temperature and stress data can then be exported to the quenching simulation part of QForm, where the quenching procedure can be simulated. But as the simulations in the thesis show, a simulation is useless without the correct parameters for the nozzles, HTC and water flow. There are some excellent points with the simulation hitting the same cooling curves, just that it is for different setups. This can most likely be explained by the lack of good concrete data on the water flows in each nozzle and the most likely misunderstanding of the HTC values. Regarding the water flow, there can be any misunderstandings between the measurements taken on the factory floor, the ones writing up the report on the testing being done,

and how it was interpreted and calculated for use in QForm. For the HTC values, having a surface temperature of over 5000 °C with aluminium in experimental cooling data does not make sense. But this was used this way in the thesis as that is how QForm showed it in their training material.

So I believe the software with better-controlled parameters and data to work with can reduce trials and errors on the quenching lines. This will have to be tried out and tested to see if the results here are just the wrong parameters and data or if the simulation software needs more work.

REFERENCES

Abdul-Jawwad, Abdul Kareem and Adnan Bashir (Feb. 2011). "A Comprehensive Model for Predicting Profile Exit Temperature of Industrially Extruded 6063 Aluminum Alloy". In: *http://dx.doi.org/10.1080/10426914.2010.505618* 26 (2), pp. 193–201. ISSN: 10426914. DOI: 10.1080/10426914.2010.505618. URL: https://www.tandfonline.com/doi/abs/10.1080/10426914.2010.505618.

ALUMINUM EXTRUSION PROCESS (2022). URL: https://bonnellaluminum.com/tech-info-resources/aluminum-extrusion-process/.

Chahare, Atish and K H Inamdar (2016). *A REVIEW ON PROCESS PARAMETERS AFFECTING ALUMINIUM EXTRUSION PROCESS*. URL: http://ijirse.com/wp-content/upload/2016/02/1425.pdf.

Deiters, T A and I Mudawar (1989). *Optimization of Spray Quenching for Aluminum Extrusion, Forging, or Continuous Casting*, pp. 9–18.

File:Extrusion force plot.png - Wikimedia Commons (n.d.). URL: https://en.wikipedia.org/wiki/Extrusion.

Flitta, I. and T. Sheppard (July 2013a). "Nature of friction in extrusion process and its effect on material flow". In: *http://dx.doi.org/10.1179/026708303225004422* 19 (7), pp. 837–846. ISSN: 02670836. DOI: 10.1179/026708303225004422. URL: https://www.tandfonline.com/doi/abs/10.1179/026708303225004422.

– (July 2013b). "Nature of friction in extrusion process and its effect on material flow". In: *http://dx.doi.org/10.1179/026708303225004422* 19 (7), pp. 837–846. ISSN: 02670836. DOI: 10.1179/026708303225004422. URL: https://www.tandfonline.com/doi/abs/10.1179/026708303225004422.

Hähnel, W, K Gillmeister, and A Kräger (2016). "Temperature management of containers". In: *Aluminium International Today* 28 (2). Copyright - Copyright Quartz Business Media Ltd Mar/Apr 2016 Document feature - Illustrations Last updated - 2022-11-12, pp. 61–63. ISSN: 1475455X. URL: https://www.proquest.com/scholarly-journals/temperature-management-containers/docview/1792581473/se-2?accountid=12870.

Hall, D D et al. (1997). *Validation of a Systematic Approach to Modeling Spray Quenching of Aluminum Alloy Extrusions, Composites, and Continuous Castings*, pp. 77–92.

Hydro extruded profiles (2022). URL: https://www.hydro.com/en-NO/aluminium/products/extruded-profiles/.

I.J., Polmeaer (1995). *Light alloys: metallurgy of light metals*. Butterworth-Heinemann. ISBN: 978-0-340-63207-9.

Jarvstrat, Niklas and Stig Tjotta (n.d.). *A Process Model for On-Line Quenching of Aluminium Extrusions*.

Llorca-Schenk, Juan, Juan Ramón Rico-Juan, and Miguel Sanchez-Lozano (July 2023). "Designing porthole aluminium extrusion dies on the basis of eXplainable Artificial Intelligence". In: *Expert Systems with Applications* 222, p. 119808. ISSN: 09574174. DOI: 10.1016/j.eswa.2023.119808.

Mackenzie, D Scott (Sept. 2020). "Heat treatment of aluminium quenching basics". In: *Thermal processing* 9. URL: $https://thermalprocessing.com/heat-treatment-of-aluminum%5C%E2%5C%80%5C%89-%5C%E2%5C%80%5C%89part-i-quenching-basics/%20https://home.quakerhoughton.com/$.

Medvedev, Alexander et al. (2020). "Innovative aluminium extrusion: Increased productivity through simulation". In: vol. 50. Elsevier B.V., pp. 469–474. DOI: 10.1016/j.promfg.2020.08.085. URL: https://www.sciencedirect.com/science/article/pii/S2351978920317832.

Pinter, Tommaso and Mohamad El Mehtedi (2012). "Constitutive equations for hot extrusion of AA6005A, AA6063 and AA7020 Alloys". In: vol. 491. Trans Tech Publications Ltd, pp. 43–50. ISBN: 9783037852507. DOI: 10.4028/www.scientific.net/KEM.491.43.

Qamar, Sayyad Zahid, A. F.M. Arif, and A. K. Sheikh (May 2004). "Analysis of product defects in a typical aluminum extrusion facility". In: *Materials and Manufacturing Processes* 19 (3), pp. 391–405. ISSN: 10426914. DOI: 10.1081/AMP-120038650. URL: https://www.researchgate.net/publication/271935668_Analysis_of_Product_Defects_in_a_Typical_Aluminum_Extrusion_Facility.

Qamar, Sayyad Zahid, Tasneem Pervez, and Josiah Cherian Chekotu (2018). "Die Defects and Die Corrections in Metal Extrusion". In: *Metals* 8.6. ISSN: 2075-4701. DOI: 10.3390/met8060380. URL: https://www.mdpi.com/2075-4701/8/6/380.

Saha, P (2000). *Aluminum Extrusion Technology*. Accession Number: 395820; OCLC: 760887055; Language: English. ASM International. ISBN: 9780871706447. URL: https://search.ebscohost.com/login.aspx?direct=true&db=nlebk&AN=395820&site=ehost-live&scope=site.

the library of manufacturing, extrusion (2022). URL: https://thelibraryofmanufacturing.com/extrusion.html.

Xu, Rong et al. (2014). "Influence of pressure and surface roughness on the heat transfer efficiency during water spray quenching of 6082 aluminum alloy". In: *Journal of Materials Processing Technology* 214 (12), pp. 2877–2883. ISSN: 09240136. DOI: 10.1016/j.jmatprotec.2014.06.027.

APPENDICES

Table .0.1: HTC table for surface temperature and liquid flux density

Surface temperature [°C]:	325	800	1750	4170	5830
Liquid flux density $[L/m^2/min]$	Heat transfer coefficient $[W/(m^2 \cdot K)]$				
20	350	350	350	350	350
40	832.288	1049.991	827.524	1352.312	1789.548
60	1314.576	1749.982	1305.048	2354.624	3229.096
80	2086.009	2449.973	1782.572	3356.936	4668.644
100	2550.99	3149.964	2260.095	4359.248	6108.192
120	2637.167	4018.72	2737.619	5361.56	7547.74
140	2658.407	4878.799	3243.729	6363.872	8987.288
160	2671.161	5165.139	3818.031	7781.095	10426.84
180	2619.127	5054.956	4629.06	9989.736	11646.03
200	2506.76	4768.778	6752.903	12409.55	12458.08
220	2358.611	4397.293	9687.196	15500.34	13270.13
240	2216.029	4010.875	10774.68	18372.54	14240.45
260	2136.605	3743.898	10791.81	19944.64	15324.69
280	2077.561	3532.425	10470.78	20665.62	16632.54
300	2006.309	3402.681	9864.143	21144.15	18006.05
320	1941.514	3301.986	9252.15	20970.16	20225.26
340	1931.354	3234.842	8625.011	19941.28	27200.69
360	1920.817	3187.448	8078.778	18496.19	27844.65
380	1908.419	3149.105	7616.219	16792.59	27356.11

Table .0.1 continued from previous page

400	1895.922	3110.761	7345.667	14671.27	26638.01
420	1871.764	3057.042	7187.057	12663.11	25672.86
440	1848.71	2989.073	7089.507	11421.81	24604.34
460	1834.448	2868.486	6997.264	10676.72	23153.61
480	1816.467	2750.699	6944.205	10176.74	21321.67
500	1805.068	2649.086	6905.62	9725.322	19296.47
520	1793.67	2552.689	6849.858	9480.572	17369.91
540	1770.662	2451.534	6775.454	9254.198	15574.46
560	1711.471	2279.605	6672.625	8972.952	14075.55
580	1617.704	2119.334	6515.157	8684.247	12824.19
600	1470.995	1961.405	6339.802	8314.601	11784.47
620	1210.109	1802.528	6106.096	7858.423	11062.24
640	952.193	1635.323	5861.898	7367.462	10410.35
660	737.572	1461.207	5607.869	6743.869	10040.09
680	558.01	1291.944	5325.338	6132.013	9669.821
700	440.817	1177.873	5042.806	5576.175	9299.557
720	362.251	1097.699	4781.003	5140.544	8935.371
740	290.144	989.515	4522.57	4779.551	8571.439
760	222.518	866.58	4264.137	4418.558	8207.506
780	158.276	743.645	4005.704	4057.564	7843.573
800	94.034	620.71	3747.271	3696.571	7479.64

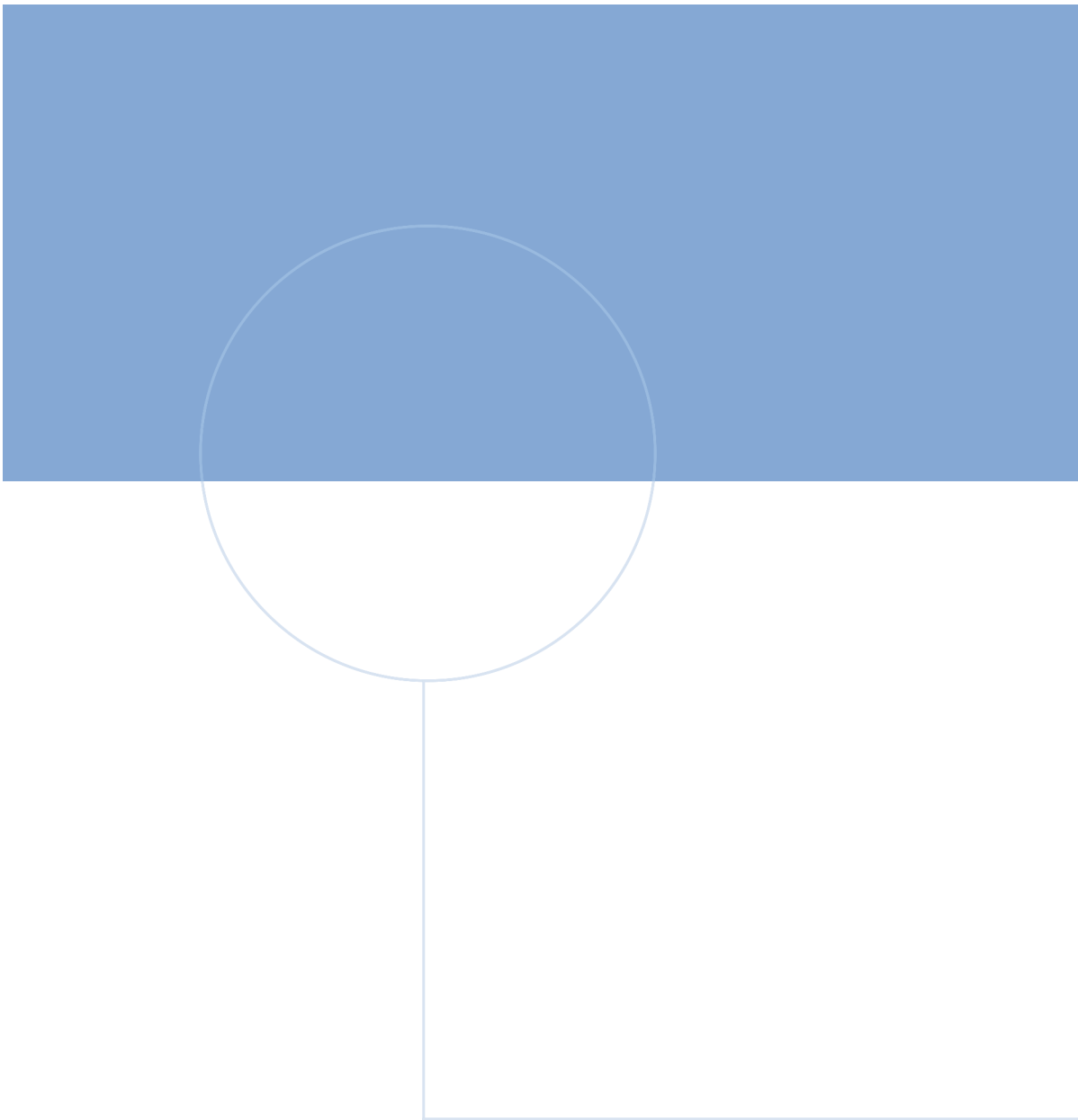

NTNU

Norwegian University of
Science and Technology